Electrical response of fractal and porous interfaces

B. Sapoval and J.-N. Chazalviel
Laboratoire de Physique de la Matière Condensée, Ecole Polytechnique, route de Saclay, 91128 Palaiseau Cédex, France

J. Peyrière
Département de Mathématiques, Université de Paris–Sud, Bâtiment No. 425, 91405 Orsay Cédex, France

(Received 22 February 1988)

The electrical response of porous electrodes is calculated in several particular cases, which permit one to approach the response of a realistic model for a porous interface. The case of nonblocking surfaces and the case of the diffusion impedance of a fractal electrode are also considered. The use of Bode diagrams is shown to provide a very simple means for calculating phase angles and algebraic values for the impedance. It is demonstrated that for a blocking deterministic Sierpiński electrode the impedance presents oscillations around a constant phase angle (CPA). Various electrochemical regimes (blocking, nonblocking, and diffusive) are considered, giving rise to a variety of exponents. For blocking electrodes it is shown that at a given frequency, the power is dissipated in certain parts of the electrodes having a characteristic size which is a direct function of frequency. The fact that the response of the system is linear permits one to relate in general the dc response to the phase angle in the blocking regime and to study certain diffusive cases. It also permits one to deal with cases very common practically where the response of a flat surface would itself exhibit a CPA. In the case of a pure diffusion impedance the response is shown to be related directly to the Minkowski-Bouligand exterior dimension of the interface through the exponent $(D-1)/2$. This approach can be generalized to any type of irregular electrode independently of its fractal character. If both diffusion and Faradaic (electrochemical) impedance play a role, a CPA response exists for a porous electrode with an exponent equal to $D-2$. We discuss various regimes in which diffusion plays a role together with Faradaic, resistive, and capacitive effects. It is shown that there is in general no relation between fractal dimension and constant phase angle except in the case of diffusion. The response of irregular electrodes is shown to be related to the fractal dimension when the electrochemical regime is local.

I. INTRODUCTION

Electrochemical batteries always exhibit a limited current output. This is due to the fact that microscopic electrochemical processes have a finite rate at the electrode-electrolyte interface and limit the current density. For years porous electrodes have been used to increase the output current because they have a large surface area. It has been observed for a long time that such electrodes do not have a simple frequency response.[1]

The equivalent circuit of a cell with planar electrodes should be made of a surface capacitance C in parallel across the Faradaic (electrochemical) resistance R_F, both being in series with the resistance of the electrolyte R_{el}. The capacitance C corresponds to the charge accumulation across the interface. The Faradaic resistance R_F represents the inverse rate of electrochemical charge transfer at the interface, for instance, in the electrochemical reaction $Fe^{3+}+e^{-}\leftrightarrow Fe^{2+}$. In the absence of such a process R_F is infinite and the electrode is said to be "blocking" or "ideally polarizable." In the presence of such a process it may happen that diffusion of the species in the liquid play a role: such a case is termed as "diffusive regime" and appears at very low frequencies only. In fact, the impedance of rough or porous electrodes is often found to be of the form

$$Z \propto (j\omega)^{-\eta} \quad \text{with } j \equiv \sqrt{-1}\ , \tag{1}$$

in series with a pure resistance which figures the resistance of the electrolyte.[1] The exponent η is such that $0<\eta<1$. This behavior is known as the constant-phase-angle (CPA) behavior. It is known that a smooth surface exhibits $\eta=1$, whereas η decreases when the roughness of the surface increases and we consider as established experimental evidence that the frequency dependence of the impedance of an electrode depends on its geometry. The understanding of this phenomenon is not complete but we think that the model of a fractal[2] surface is a fruitful approach that we want to examine in this paper. A nonfractal interpretation of the CPA interface impedance considering an electrode made of identical horn-shaped pores has also been proposed.[3]

Le Méhauté first proposed to consider a rough or porous interface as a fractal interface and he first tried to relate the exponent η with the fractal dimension D of the interface. He proposed the word "fractance" for the description of such an impedance but presented a theory which cannot be considered as well justified.[4,5] Yet, such

a connection between fractal geometry and power-law behavior was appealing and several studies have been devoted to this subject.[6–14] These works have mainly considered the properties of a "blocking" or "ideally polarizable" fractal electrode for which the Faradaic resistance R_F is infinite. Liu has given a calculation for the "Cantor-bar electrode."[7] In the limit of low-enough frequencies it is equivalent to a hierarchical lumped network for which the impedance presents a power-law behavior with

$$\eta = 3 - D \ . \tag{2}$$

More recently another special case, the "modified Sierspiński electrode" has been proposed, for which the calculation can be made exactly, i.e., without the approximation of a lumped circuit.[15] The "modified Sierspiński electrode" (modified SE) is the metallic electrode shown in Fig. 1. It has indeed an infinite surface area included in a finite volume. A cross section of the electrode is a "modified Sierpiński carpet" for which the interface has the usual fractal dimension in the plane $D_p = \ln N / \ln \alpha$. The electrode is a cylinder whose surface has the fractal dimension $D = 1 + D_p$. The study in Ref. 15 was exact except for the neglect of "edge effects" which are important only at very high frequency. In that work "exact" analytical expressions were calculated numerically. For $D > \frac{5}{2}$ the electrode has essentially no impedance if it possesses infinitely small pores (mathematical fractal) but a real electrode with finite smaller pores would behave as a capacitor at low frequency and as a Warburg impedance at high frequency though it is a blocking electrode. For fractal dimensions smaller than $\frac{5}{2}$, numerical values of the phase angle obtained at low frequencies from "exact" expressions agree remarkably well with relation (2).[15] Very recently, it was shown that the use of Bode diagrams permits one to calculate very simply the phase angle and approximate expressions for the value of the impedance.[16]

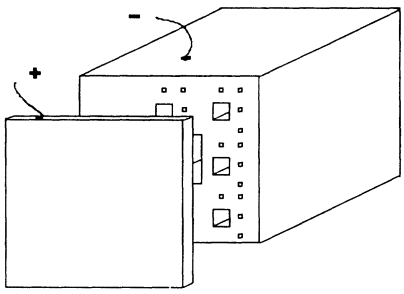

FIG. 1. Picture of the "finite modified Sierpiński electrode" in front of a planar counter electrode. The fractal object that we consider is made through a decimation process. At the first step a square pore of side a_0 is made in the electrode of side a. Then, at each step, N smaller pores of side a_0/α are added around a pore of a given size and so on. Here $N=5$ and $\alpha=3$. The length of the electrode is L. We consider a case where (1) the planar electrode is very near the fractal electrode so that one can neglect the resistance of the thin layer of electrolyte between the two electrodes, (2) the metal is supposed to have zero resistivity and the external surface is coated with an insulating material so that we neglect conduction through this surface, and (3) the bottom of each pore is insulating. All the pores are linked in parallel and the admittance is simply the sum of the admittances of all the pores.

It is remarkable that the exponent seems to satisfy relation (2) exactly although the geometry of Fig. 1 could be regarded as basically different from the Cantor-bar geometry studied by Liu.[7] One might even conclude that relation (2) is a good candidate if one wants to relate CPA to fractal dimensions. One must, however, keep in mind that Sierpiński electrodes with $D > \frac{5}{2}$ are exact counterexamples to this same relation and other counterexamples exist.[13,17] Also the Sierpiński electrodes can be considered as being far from real systems because they possess very narrow pores. As a model of real electrodes the Cantor-bar geometry can also be criticized because it also possesses very narrow pores and it is in principle of infinite size. On the other hand, a real rough surface has properties which are different in the directions parallel and perpendicular to the surface. In that sense self-affine fractals should provide a better description of the geometry of real surfaces. By calculating the impedance of a self-affine electrode derived from the Cantor-bar electrode in a lumped-circuit approximation, Kaplan *et al.* show that there exists no universal relation in which η is simply a function of D.[13] Up to now this result is demonstrated only in the lumped-circuit approximation.

One should call attention to the fact that the fractal dimension of a surface is not sufficient in itself to solve the problem. Consider, for example, a system for which we have the same surface but we "invert" (i.e., exchange the location of) the metal and the electrolyte. In the case of a SE one has to deal essentially with one pore of infinite capacitance per unit length and edge effects are dominant. There exist, however, geometries for which one can exchange metallic volumes with electrolyte volumes and keep the same frequency dependence. Such a case is the case of the "inverse Cantor bar" for which relation (2) is satisfied.[12]

Halsey has proposed a more general approach for the impedance of rough surfaces.[9,10] His approach permits one, in principle, to deal with the "edge effects" which are of primary importance at very high frequency. The calculation shows also a frequency region in which CPA behavior is observed. In his perturbative approach the impedance is calculated to one-loop order as a function of fluctuations in the height of the metallic surface. In a particular case Halsey finds the relation $\eta = 5 - 2D$ in the first-order approximation but no firm proposal can yet be established to higher order in perturbation theory. "Edge effects" would also dominate the example of a cylindrical electrode made of a single pore of fractal cross section like a Koch island because the capacitance for the mathematical fractal would be infinite.

Until very recently, no experiment has been able to confirm or to contradict these proposals. There are two reasons for that. First, it is difficult to measure the fractal dimension of real objects imbedded in three-dimensional (3D) space. Second, one has to control the electrochemical regime itself. It is, however, of interest

to confirm or to select between these conflicting results because from a good relation one should eventually be able to determine a fractal dimension from impedance measurements. Nyikos and Pajkossy claimed to have proven experimentally that $\eta=(D-1)^{-1}$ for a Koch electrode (that is, an electrode whose projected surface is the triadic Koch curve).[18] It will be shown here that the argument that the impedance of a fractal electrode is an extensive quantity, that they use in their theory, is not true in general. Recently, Bates and Chu have performed a careful study of metal–to–liquid-electrolyte impedance together with a detailed study of the surface profile.[19] They conclude that there is no connection between the fractal geometry of the electrode and the impedance exponent, but this again is perhaps related to edge effects or to the difficulty to analyze experimentally fractal profiles. Very recently Keddam and Takenouti have studied the frequency response of a two-dimensional Koch electrode made of anodized aluminum.[20] They have studied the potential distribution in that blocking case and have demonstrated that the equipotential lines in the electrolyte penetrate the fractal object in a nonuniform manner. This idea was independently discussed by Wang.[21]

These works, except Ref. 16, have so far considered only "blocking" electrodes: neither the Faradaic effects nor diffusion impedance has been taken care of. The diffusion impedance of a fractal interface has been calculated by Nyikos and Pajkossy in the particular case of a Koch electrode.[22] They have demonstrated in this case that

$$\eta=(D-1)/2 \ . \tag{3}$$

Such a result was suggested by de Gennes in a somewhat different context.[23] We shall give a general demonstration of that result and we will show that the diffusion regimes give in principle a new tool to measure surfaces, whether fractal or not.

To summarize the present situation, we know that there exist fractal electrodes for which there is a direct relation between the frequency exponent and the fractal dimension, but there also exist fractal electrodes for which such a relation does not hold. The purpose of this paper is to help in clarifying this matter. For that we first recall in Sec. II how the use of Bode diagrams permits one to calculate readily the impedance of Sierpiński electrodes. We show that at a given frequency the power is dissipated in pores of a given characteristic size. We apply the same method to what we call "generalized" self-affine Sierpiński electrodes and we discuss the parallel branching of spheroidal pores for which we show that CPA is obtained only when the surface is nonfractal.

As we will show in the following, in an electrochemical system there exist essentially two scale lengths at a given frequency. If we want to describe "fractal" objects by a dimension, it is reasonable to use a concept of dimension which is based on the idea of "neighboring" and we want this concept to have a wide applicability. We propose in Sec. III to use a definition of the dimension based upon the evaluation of the amount of electrolyte located within a given distance from the interface. This leads us to the mathematical concept known as "exterior Minkowski-Bouligand dimension" and we will show in the study of diffusion that it has indeed a profound physical meaning. In particular, it permits one to describe the impedance of any irregular, rough or porous, fractal or nonfractal interface in the diffusive regimes.

The Bode-diagram method is systematically applied in this paper to the study of a number of geometries and electrochemical regimes. For this reason we discuss in Sec. IV its mathematical basis, the effect of disorder, and the linear-response aspects of that question.

In Sec. V we discuss the series-parallel branching. We show that also in that case, the electrical power is dissipated at a given frequency in pores of a given characteristic size. The Cantor-bar electrode is shown to yield the same algebraic value for the impedance as a SE. We find that a true self-similar tree structure does not exhibit CPA if the electrolyte is inside the tree. The same result applies to a series-parallel branching of spheroidal pores.

Section VI is devoted to the approximate study of a generalization of spherical-pore electrodes to porous electrodes for which we show that parallel branching may be the cause of CPA. We then discuss in Sec. VII the frequency dependence of the impedance for the same electrodes in presence of Faradaic response of the interface and show that the exponent is not modified but that the frequency range of observation is reduced. In Sec. VIII we consider approximately the frequency dependence of the edge effects which are important at high frequency and we finally show how the same Bode diagrams permit one to discuss diffusion effects or mixed effects of diffusion, resistivity of the electrolyte, Faradaic resistance, and interface capacitance.

We first review briefly the usual model for the electrical response of an electrical cell with planar electrodes to a small voltage excitation of frequency ω. There exist basically four elements in the equivalent electrical circuit of such a cell. They represent first the resistance of the electrolyte $R_{\rm el}$ proportional to the electrolyte resistivity ρ and depending upon the geometry of the cell. Secondly, there is the surface capacitance $C=\gamma S$ proportional to the surface area and to the specific capacitance per unit area γ. For a blocking electrode there is a "natural" length in the problem

$$\Lambda(\omega)=(\rho\gamma\omega)^{-1} \tag{4}$$

and edge effects will appear when $\Lambda(\omega)$ is smaller than the distances present in the objects. This occurs at high frequencies. For a nonblocking electrode there is also a Faradaic resistance $R_F=rS^{-1}$ where r is inversely proportional to the specific exchange current density and finally a diffusion impedance which is of importance at very low frequency. They are shown in Fig. 2(a). A given electrochemical interface is characterized by the frequency ω_f

$$\omega_f=(\gamma r)^{-1} \ . \tag{5}$$

Diffusion, if present, also introduces a scale length $\Lambda_{\mathcal{D}}=(\mathcal{D}/\omega)^{1/2}$ which is the diffusion length at the fre-

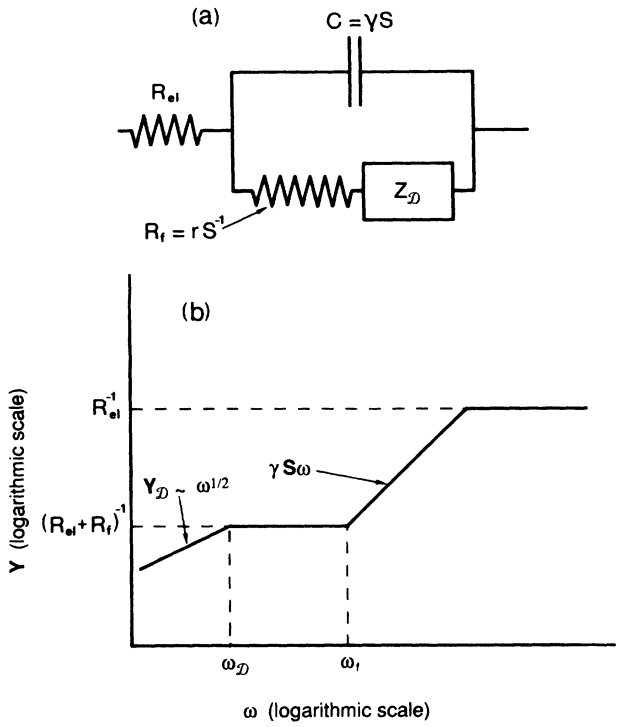

FIG. 2. (a) Equivalent circuit of a planar electrode in the small voltage linear regime. (b) Schematized Bode diagram of that circuit.

quency ω with a diffusion coefficient $\mathcal{D}$. There exists a diffusion impedance $Z_{\mathcal{D}} \propto (j\omega)^{-1/2}$ in series with the Faradaic resistance. This will be discussed in detail in Sec. IX where we also show that taking into account the diffusion and the Faradaic impedance we obtain a value of the exponent $\eta = D-2$ and that this regime is governed by a scale length $\Lambda'(\omega) = (rc\omega)^{-1}$.

In this paper we successively examine various geometries and various electrochemical situations. Several conclusions of different purpose are obtained. Some results are general, some are not. To avoid confusion we suggest that the reader refer when necessary to the conclusions where the essential results are listed.

II. "MODIFIED SIERPIŃSKI ELECTRODE" AND PARALLEL STRUCTURES IN THE BODE DIAGRAM

In the following we will discuss the impedance of fractal electrodes using the Bode diagrams. A Bode diagram (BD) is a plot of $\ln | Y |$ as a function of $\ln\omega$. The BD of a planar electrode is essentially made from straight lines as shown in Fig. 2(b). There are four regions starting from ultralow frequency. First there is a straight line of slope $\frac{1}{2}$ representing diffusion admittance up to a frequency

$$\omega_{\mathcal{D}} \sim 1/\mathcal{D}(cr)^2 , \tag{6}$$

where the diffusion impedance is equal to the Faradaic resistance r [c is an equivalent volumic capacitance density defined in Sec. IX, Eq. (63)]. Above $\omega_{\mathcal{D}}$ the horizontal line represents the Faradaic resistance up to the frequency ω_f. It is followed by a line of slope 1 representing the admittance of the surface capacitance, and finally a second horizontal line representing the resistance of the electrolyte.

In the geometry shown in Fig. 1 all the pores are linked in parallel and the admittance is simply the sum of the admittances of all the pores. We have to calculate the impedance of an infinite square hole of side a_n taking into account the resistivity ρ of the electrolyte and the surface impedance. This can readily be done by using de Levie's method.[24] Apart from very high frequencies for which edge effects have to be considered, equipotential lines can be approximated by planes. If, inside a pore, the electric potential and current vary as $V(x,t) = V(x)\exp(j\omega t)$ and $I(x,t) = I(x)\exp(j\omega t)$, we have (here we neglect diffusion effects)

$$-dV(x) = (\rho/a_n^2) I(x) dx , \tag{7}$$

$$-dI(x) = 4(j\gamma\omega + r^{-1}) a_n V(x) dx . \tag{8}$$

We have then

$$d^2V(x)/dx^2 = (4\rho/a_n)(j\gamma\omega + r^{-1})V(x) = (\lambda_n)^{-2}V(x) . \tag{9}$$

The length $|\lambda_n|$ is the characteristic attenuation length inside the pore. The solution of this last equation is a linear combination of $\exp(x/\lambda_n)$ and $\exp(-x/\lambda_n)$ which satisfy the boundary condition $V(x=0) = V_0$, where V_0 is the applied voltage and $I(x=L) = 0$. The bottom of the pore is supposed to be insulating which makes little difference for narrow pores. The admittance of a single pore is obtained by using relation (7):

$$Y_n = 2(a_0/\alpha^n)^{3/2}(\rho r)^{-1/2}(1 + j\omega/\omega_f)^{1/2} \times \tanh[2(\rho L^2 \alpha^n / a_0 r)^{1/2}(1 + j\omega/\omega_f)^{1/2}] . \tag{10}$$

The total admittance is the sum of the admittances of all the pores:

$$Y = \sum_{n \geq 0} N^n Y_n . \tag{11}$$

If the length of the electrode is infinite the admittance of all the pores is proportional to $(1 + j\omega/\omega_f)^{1/2}$ and the frequency dependence is not related to the fractal dimension. For finite length that we discuss from now on, the admittance is purely resistive at very low frequencies ($\omega \ll \omega_f$). It is purely capacitive in the low-frequency range, where

$$\omega > \omega_f \text{ and } 4\gamma\omega\rho L^2\alpha^n/a_0 < 1 . \tag{12}$$

In this range the argument of the hyperbolic tangent is small. At high frequency,

$$\omega > \omega_f \text{ and } 4\gamma\omega\rho L^2\alpha^n/a_0 > 1 , \tag{13}$$

the pore behaves as a diffusion impedance proportional to $(j\omega)^{-1/2}$ although it is blocking. At still higher frequencies edge effects have to be considered and this will be discussed in Sec. VIII. The corresponding BD is shown in Fig. 3(a).

We first discuss the case of a blocking or a nearly blocking electrode for which ω_f is very small so that we consider only the two regimes (12) and (13). At low frequency the admittance is simply due to the capacitance of the pore

$$Y_n = 4j\omega\gamma a_0 L/\alpha^n \ . \tag{14}$$

In the higher-frequency range (13) the admittance has the value

$$Y_n = 2^{1/2}(a_0/\alpha^n)^{3/2}(\gamma\omega/\rho)^{1/2}(1+j) \ . \tag{15}$$

Then a pore has a characteristic frequency ω_n given by

$$\omega_n = a_0/4\gamma\rho L^2\alpha^n \ , \tag{16}$$

where the argument of the hyperbolic tangent in (10) is of modulus 1 and where the value of the modulus of the admittance has a characteristic value $Y_{c,n}$ of the order of

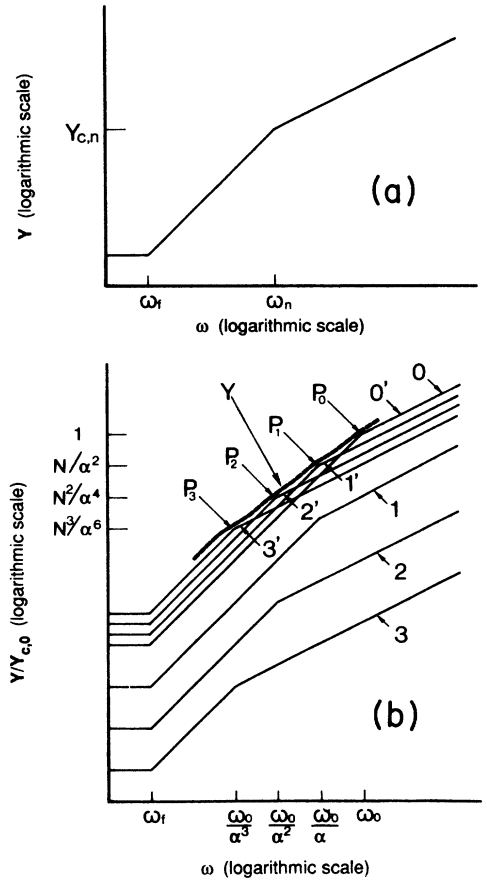

FIG. 3. Bode diagram description of the impedance of the Sierpiński electrode. (a) Schematic Bode diagram of a single pore showing the three frequency regimes. Notice the "shoulder" at the characteristic frequency ω_n given by Eq. (16). (b) Shows the construction of the Bode diagram of the entire electrode from the Bode diagram of the individual pores. The thick line has an average slope equal to $\eta = 2 - \ln N/\ln\alpha$. The small oscillation is real. It is due to the finite steps in the decimation process as discussed in Sec. IV. At very low frequency the admittance is constant. Between ω_f and ω_0 one observes CPA behavior. Above ω_0 an $\omega^{1/2}$ behavior is predicted.

$$Y_{c,n} = a_0^2/\alpha^{2n}\rho L \ . \tag{17}$$

Because all pores are linked in parallel the BD of the electrode can be obtained very simply by adding the BD of the pores. This is done as explained below. Consider the largest pore $n=0$. It has a characteristic frequency $\omega_0 = a_0/4\gamma\rho L^2$ with admittance $Y_{c,0} = a_0^2/\rho L$. It has a BD shown as curve 0 on Fig. 3(b). The next smaller pores ($n=1$) have a characteristic frequency $\omega_1 = \omega_0/\alpha$ and an admittance $Y_{c,1} = Y_{c,0}/\alpha^2$. Their BD is shown as curve 1. Because they are in number N their total contribution to the admittance is curve 1′ obtained by a vertical translation of $\ln N$ is the BD. The next smaller pores have $\omega_2 = \omega_0/\alpha^2$ and an admittance at ω_2 equal to $Y_{c,0}/\alpha^4$, their BD is curve 2 and they contribute as curve 2′ to the admittance of the electrode, and so on. The admittance of the electrode is the sum of curves $0', 1', 2', \ldots$. It is shown approximately as curve Y_T. Because of the logarithmic structure of the Bode diagram one observes that at frequency ω_0 the admittance is governed essentially by $Y_{c,0}$, at frequency ω_1 by $NY_{c,1}$, at ω_2 by $N^2Y_{c,2}$ so that the curve Y_T goes essentially from the points (P_0) to (P_1) to (P_2) with a small oscillation. This has two consequences. First the behavior of Y_T as a function of ω is, apart from the small oscillation, a straight line of slope η

$$\eta = [(\ln Y_0 - \ln(NY_0\alpha^{-2})]/(\ln\omega_0 - \ln(\omega_0\alpha^{-1})]$$
$$= 2 - (\ln N/\ln\alpha) = 3 - D \ . \tag{18}$$

This argument gives a slightly approximate but direct proof of the existence of CPA. Of course, this is only a result on the modulus of the admittance. But behavior of the phase angle and modulus are closely related through linear-response theory. An exact result on the impedance will be given in Sec. IV.

The same argument also gives an approximate value of the impedance itself at a given frequency ω: At this frequency the impedance is dominated in first approximation by the pores of characteristic frequency ω. There are $N^{n(\omega)}$ such pores where $n(\omega)$ is given by relation (16)

$$n(\omega) \sim \ln(a_0/4\gamma\rho L^2\omega)/\ln\alpha \ . \tag{19}$$

The admittance of the electrode at that frequency is then essentially

$$|Y_T| \sim (a_0^2/\rho L)(N/\alpha^2)^{n(\omega)} \ . \tag{20}$$

Using (19), one finds

$$|Y_T| \sim (a_0^2/\rho L)(a_0/\gamma\rho L^2\omega)^{D-3} \ . \tag{21}$$

As a consequence, the modulus of the admittance has indeed a power-law dependence. A constant phase angle is then a consequence of linear response. The function (21) is a nontrivial function of a_0, ρ, γ, L and ω. In particular, the admittance of such an electrode is not a simple square function of the size of the object: Y_T varies as a_0^{D-1} and L^{5-2D}. This result, exact for this particular case, contradicts the hypothesis of Nyikos and Pajkossy that Y scales as the surface of the object.[8]

The same argument leads us to an important remark: Because at a given frequency ω the admittance is dom-

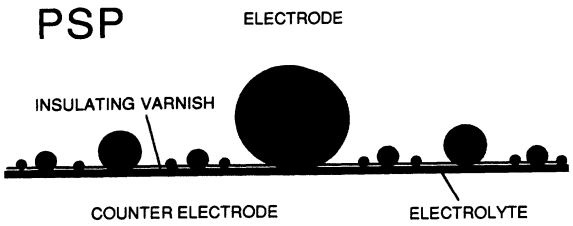

FIG. 4. Parallel spherical pores (PSP). The electrolyte is shown in gray. The openings of the spherical pores are supposed to be smaller than the radius of the pores but of the same order of magnitude. They are supposed to scale the same way.

inated by the pores of characteristic frequency ω, the energy is dissipated in those pores. On such fractal interfaces the power dissipation is nonuniform. Also, it is obvious from Fig. 3 that the nonblocking character of the interface plays no role in the value of η as long as the frequency is larger than ω_f. Below ω_f the impedance is purely resistive. Then the effect of the existence of a Faradaic reaction is to limit the frequency range in which relation (2) is satisfied to frequencies ω such that $\omega_f < \omega < \omega_0$. This constitutes an "exact" result which contradicts the generality of the prediction that a "dissipative" surface would behave differently from a nondissipative surface.[4]

It is easy to find a more exact expression taking care of neighboring pores but that will not change η. This will be done in Sec. III. The above result is valid only if the summation converges. We must make a distinction between "mathematical" fractals for which there is an infinite hierarchy of smaller and smaller pores and "physical" fractals in which the smaller pores are finite. In the first case the number of pores of side a_0/α^n increases as N^n, whereas the admittance of each pore behaves as $\alpha^{-3n/2}$ from relation (10). So the total admittance is infinite if $N > \alpha^{3/2}$ that is $D > \frac{5}{2}$. For a physical fractal with $D > \frac{5}{2}$ the behavior will be dominated by the smaller pores and the result will depend on the size of the smaller pores as compared with the frequency. For fractal dimensions smaller than $\frac{5}{2}$ it is clear from Fig. 3 that there are two frequency domains separated by ω_0. Above that frequency the value of η is $\frac{1}{2}$.

Before going to different geometries we consider the case of what we call a "generalized" Sierpiński electrode." A generalized Sierpiński electrode is an electrode similar to that in Fig. 1, where the length of the pores, instead of being constant, also scales (either as the side or differently). The first pore has a length L, the next pores have a length L/α_z, and so on. This case can be considered as more physical than the previous models of a surface because thinner pores can be shorter than thicker pores. A pore has now an impedance given by a relation similar to (10) but where L is replaced by L/α_z^n,

$$Y_n = 2(a_0/\alpha^n)^{3/2}(\rho r)^{-1/2}(1+j\omega/\omega_f)^{1/2} \times \tanh[2(\rho L^2\alpha^n)/\alpha_z^{2n}a_0 r)^{1/2}(1+j\omega/\omega_f)^{1/2}] . \quad (22)$$

The characteristic frequency is $\omega_n = a_0\alpha_z^{2n}/4\gamma\rho L^2\alpha^n$, where the argument of the hyperbolic tangent in (22) is of modulus 1. At ω_n the value of the modulus of the admittance has a characteristic value $Y_{c,n}$ of the order of $Y_{c,n} = (a_0^2/\rho L)(\alpha_z/\alpha^2)^n$. The consideration of the BD in this case gives

$$\eta = (\ln N + \ln\alpha_z - 2\ln\alpha)/(2\ln\alpha_z - \ln\alpha) , \quad (23)$$

but, as we shall see in Sec. III this is not simply a function of the dimension of the object.

Finally we consider the parallel branching of spheroidal pores (PSP) as shown in Fig. 4. The entrance of the spheroidal cavities is supposed to be large enough so that edge effects can be neglected. The size b_n of the cavity scales with a factor α^{-n}. We approximate the resistance of each cavity at stage n by $R_n \sim \rho/b_n \sim (\rho/b_0)\alpha^n$ and the capacitance by $C_n \sim \gamma b_n^2 \sim \gamma b_0^2 \alpha^{-2n}$. The number of cavities of rank n is N^n and the cavities are accessed in parallel from the electrode front surface (this actually is close to a generalized Sierpiński electrode with $\alpha = \alpha_z$). It is straightforward from a Bode plot that the parallel circuit of Fig. 4 yields a CPA behavior, with exponent $\eta = \ln(N/\alpha)/\ln\alpha$, in the frequency range $1/R_0C_0 \ll \omega \ll 1/R_\mu C_\mu$ or equivalently $(\rho\gamma b_0)^{-1} \ll \omega \ll (\rho\gamma b_\mu)^{-1}$. This, however, occurs only when $\alpha < N < \alpha^2$, the condition at which the surface is finite even for infinite decimation. Using the Minkowski-Bouligand dimension defined below one finds under these conditions that $D = 2$ in that case. When N and α are such that the electrode is fractal with an infinite area then the admittance is essentially that of the smallest pores and no CPA behavior is found.

III. DIMENSION

Since we consider electrodes of which the front face is varnished, we are not interested in the position of pores, but only in their repartition. This leads to try to compare the CPA exponent to an index which has been introduced by Grebogi *et al.* under this name of "exterior dimension" in the spirit of the Minkowski-Bouligand unilateral dimension.[25] This notion has been studied by Tricot, who called that index "exchange coefficient."[26] Here exterior means exterior to the electrode.

Let us now define this coefficient. Let ε be a (small) positive length. Let V_ε denote the volume of electrolyte which lies within distance ε from the electrode. Then

$$D = \lim_{\varepsilon\to 0}(3 - \ln V_\varepsilon/\ln\varepsilon) . \quad (24)$$

If this limit does not exist, take the least upper bound. This definition is illustrated in Fig. 5. It is known that D may differ from the fractal dimension of the common boundary of the electrode and of the electrolyte. In that case exchanging the electrode and the electrolyte can give a different value for the index for specific geometries.[27]

We now compute this dimension in the case of generalized Sierpiński electrodes. We have N^n pores of length $L\alpha_z^{-n}$ and of side $a_0\alpha^{-n}$. As previously, the fact that the electrode occupies a finite volume implies $N \le \alpha^2$. Let ε be a small positive length and ν the integer defined by the

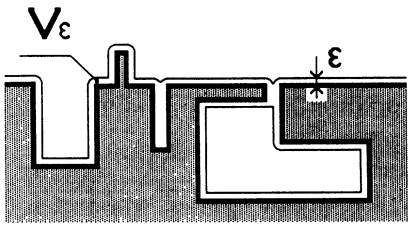

FIG. 5. Definition of the "exterior Minkowsky-Bouligand dimension." The contour of the electrode is the solid line. The electrode is shown in gray. The contour is "fattened" in the electrolyte by taking all the points of distance smaller than ε to the electrode (thin line). The volume $V(\varepsilon)$ is proportional to ε^{3-D} for an ordinary fractal surface.

inequalities $\alpha^{-\nu-1}a_0<\varepsilon/2<\alpha^{-\nu}a_0$; we then have

$$V_\varepsilon\sim\sum_{n=\nu}^{\infty}N^n a_0^2L(\alpha^2\alpha_z)^{-n}+4\varepsilon\sum_{n=0}^{\nu-1}N^n a_0L(\alpha\alpha_z)^{-n}\ , \quad (25)$$

with an error, due to edge effects, of the order of magnitude of ε. Two alternatives may occur.

First, $N>\alpha\alpha_z$. Then the second term is of the order of magnitude of $\varepsilon N^\nu a_0L(\alpha\alpha_z)^{-\nu}$ and the first term is equivalent to $N^\nu a_0^2L(\alpha^2\alpha_z)^{-\nu}$. Remembering that $\nu\approx\ln(a_0/\varepsilon)/\ln\alpha$, we get $V_\varepsilon\approx\varepsilon^2\varepsilon^{-\ln(N/\alpha_z)/\ln\alpha}$, and so

$$D=1+(\ln N-\ln\alpha_z)/\ln\alpha\ . \quad (26)$$

If $\alpha_z=1$ we recover $D=1+\ln N/\ln\alpha$; note that if $\alpha_z=\alpha$ we have a true self-similar structure and D is the self-similarity dimension $\ln N/\ln\alpha$ but this N must simultaneously satisfy $N<\alpha^2$ to permit construction in a finite volume.[15] This imposes $N=\alpha^2$ and $D=2$ in this case. If a finite volume is not required D is equal to $\ln N/\ln\alpha$. Comparison of relations (23) and (26) shows that there is no relation between the dimension and the phase angle in the case of generalized Sierpiński electrodes. This fact was already pointed out for Cantor-bar structures.[12]

In the second case where $N<\alpha\alpha_z$, the second term in (25) is of the order of ε, whereas the first one is smaller. We then have $V_\varepsilon\approx\varepsilon$ and therefore $D=2$. When $N=\alpha\alpha_z$, we have also $D=2$. An analogous calculation of D for PSP (Fig. 4) gives $D=\ln N/\ln\alpha$ if $N>\alpha^2$ and $D=2$ if $N<\alpha^2$.

IV. PARALLEL BRANCHING

When dealing with the previous examples of electrodes or of hierarchical circuits, the admittance Y of the system, which is the sum of the series of the admittances of the subsystems, has the form

$$Y(\omega)=\sum_{n=0}^{\infty}\lambda^{-n\eta}y(\omega\lambda^\eta)\ , \quad (27)$$

where the number λ is determined by the geometry and y is the admittance of one particular subsystem taken as reference.

Let us consider the example of the generalized Sierpiński electrodes in the blocking case. The admittance of a square pore of side a_0 and length L is, in the regime $\omega>\omega_f$,

$$y(\omega)=\rho^{-1}a_0^2A(j\omega)^{1/2}\tanh[AL(j\omega)^{1/2}]\ , \quad (28)$$

where $A=2(\gamma\rho/a_0)^{1/2}$ and $(j\omega)^{1/2}$ is the principal determination of the square root. For a pore of side a_0/α^n and length L/α_z^n, the admittance is

$$y_n(\omega)=\rho^{-1}a_0^2\alpha^{-3n/2}A(j\omega)^{1/2}\tanh[AL\alpha^{n/2}\alpha_z^{-n}(j\omega)^{1/2}]$$
$$=\alpha^{-2n}\alpha_z^n y(\alpha^n\alpha_z^{-2n}\omega)\ . \quad (29)$$

Therefore the admittance of N^n such pores in parallel is $\lambda^{-n\eta}y(\lambda^\eta\omega)$ where $\lambda=\alpha/\alpha_z^2$ and $\eta=\ln(N\alpha_z/\alpha^2)/\ln(\alpha_z^2/\alpha)$. So, for a generalized Sierpiński electrode, the admittance has the form (27) with η given by Eq. (23).

Usually, as in the previous example, the function y of the frequency ω can be extended as an holomorphic function to an angular sector of the complex plane. Moreover, $y(-j\omega)$ is real. We are going to prove that, under suitable conditions on y, $Y(\omega)$ behaves as $\omega^\eta u(\ln\omega)$ when ω is small if $\lambda>1$ (when ω is large if $\lambda<1$). The function u is a periodic function with period $\ln\lambda$. This oscillation factor, which is visible on the Bode diagram of Fig. 3(b), is due to the rigidity of the hierarchical construction. Later, we shall explain how to get rid of it.

We will now make some precise statements. Let S be a closed angular sector of the complex plane: $S=\{z\in\mathbb{C}|\theta_1<\arg z<\theta_2\}$. Let y be a continuous function from S to $\mathbb{C}$, holomorphic on S, and such that there exist three positive constants C, β, and δ (with $\beta<\delta$) so that

$$|y(z)|\le C\min\{|z|^\beta,|z|^\delta\}\ \forall z\in S \quad (30)$$

(for SE, $\beta=\frac{1}{2},\delta=1$). This means that the BD of $y(z)$ exhibits a "shoulder" as shown, for example, in Fig. 3(a). Let us now consider the case where λ is a number larger than 1 and η a number in the open interval (β,δ). Let us set

$$Y(z)=\sum_{n\ge0}\lambda^{-n\eta}y(z\lambda^n)\ . \quad (31)$$

This series converges uniformly on compacts of S, so its sum Y is a continuous function on S, holomorphic on S. Let B denote the strip $B=\{w\in\mathbb{C}|\theta_1<\mathrm{Im}w<\theta_2\}$. The exponentiation mapping, $w\to e^w$, is a one-to-one mapping from B onto S. We define a function $u(w)$ on B:

$$u(w)=e^{-\eta w}\sum_{n\in\mathbb{Z}}\lambda^{-n\eta}y(\lambda^n e^w)\ . \quad (32)$$

It is easy to check that this series converges uniformly on compacts of B. So the function u is continuous on B, holomorphic on the interior of B. Moreover, this function u is easily seen to be periodic of period $\ln\lambda$. We have, for any $k>0$,

$$Y(z\lambda^{-k})=\sum_{n\ge0}\lambda^{-n\eta}y(z\lambda^{n-k})$$
$$=\lambda^{-k\eta}\sum_{n\ge0}\lambda^{(k-n)\eta}y(z\lambda^{n-k})$$
$$=\lambda^{-k\eta}\sum_{n\ge-k}\lambda^{-n\eta}y(z\lambda^n)\ . \quad (33)$$

Hence,

$$z^{\eta}u(\ln z)-\lambda^{k\eta}Y(z\lambda^{-k})=\sum_{n<-k}\lambda^{-n\eta}y(z\lambda^{n}) ,$$

so

$$|z^{\eta}u(\ln z)-\lambda^{k\eta}Y(z\lambda^{-k})|\le C\sum_{n>k}\lambda^{n\eta}|z\lambda^{-n}|^{\delta} \le C|z|^{\delta}\lambda^{(k+1)(\eta-\delta)}/(1-\lambda^{\eta-\delta}) . \tag{34}$$

Now, if we set $\omega=z\lambda^{-k}$, we get

$$|\omega^{\eta}u(\ln\omega)-Y(\omega)|\le C'|\omega|^{\delta} , \tag{35}$$

which is a bit better than $Y(\omega)\sim\omega^{\eta}u(\ln\omega)$ for small ω's. The case $\lambda<1$ is treated similarly. In the case of the generalized Sierpiński electrodes, it is easy to determine the Fourier coefficients of u: They decrease rapidly and the mean value of u is much larger than the other coefficients. This explains the small oscillations appearing on the computed Bode diagrams.

The above theorem can be generalized to a random situation. Let us consider an electrode with square pores of constant length L. But this time we suppose that the number of pores of sides between a_0/λ_2 and a_0/λ_1, $(1<\lambda_1<\lambda_2)$, is a Poisson variable of mean

$$\int_{\lambda_1}^{\lambda_2}\lambda^{\kappa-1}d\lambda . \tag{36}$$

Let us denote $\overline{M}$ the measure on $[1,+\infty)$ whose density with respect to the Lebesgue measure is $\lambda^{\kappa-1}$ and M the random Poisson measure whose intensity is $\overline{M}$.

Then, if $y(\omega)$ stands for the admittance of a pore of length L and side a_0, the admittance of the electrode is the random function

$$Y(\omega)=\int_1^{\infty}\lambda^{-2}y(\lambda\omega)dM(\lambda) . \tag{37}$$

So we have

$$\langle Y(\omega)\rangle=\int_1^{\infty}\lambda^{\kappa-3}y(\lambda\omega)d\lambda =\omega^{2-\kappa}\int_{\omega}^{\infty}\theta^{\kappa-3}y(\theta)d\theta , \tag{38}$$

provided $\kappa<\frac{3}{2}$ (which ensures that the integral converges). If the $\kappa\ge\frac{3}{2}$, the admittance is infinite.

If $\kappa<1$, there is no CPA behavior. If $1<\kappa<\frac{3}{2}$, the integral $\int_0^{\infty}\theta^{\kappa-3}y(\theta)d\theta$ converges, therefore $\langle Y(\omega)\rangle \approx\omega^{2-\kappa}$ for small ω's.

So the mean value of $Y(\omega)$ has a CPA behavior. Indeed this statistical approach is not limited to such pores. The above analysis applies to more general cases, for instance, where

$$Y(\omega)=\int_1^{\infty}\lambda^{-\xi}y(\lambda\omega)dM(\lambda) . \tag{39}$$

For instance, parallel juxtaposition of hyperbranched spherical pores as defined in Sec. VI could be considered this way.

For a SE we have also

$$V_{\varepsilon}\approx\int_1^{a_0/2\varepsilon}4a_0L\varepsilon\lambda^{-1}dM(\lambda)+\int_{a_0/2\varepsilon}^{\infty}a_0^2L\lambda^{-2}dM(\lambda) , \tag{40}$$

$$\langle V_{\varepsilon}\rangle\approx\int_1^{a_0/2\varepsilon}a_0L\varepsilon\lambda^{\kappa-2}d\lambda+\int_{a_0/2\varepsilon}^{\infty}a_0^2L\lambda^{\kappa-3}d\lambda \approx\varepsilon^{2-\kappa} . \tag{41}$$

This expression of $\langle V_{\varepsilon}\rangle$ does not strictly enable us to determine the dimension of the electrode through Eq. (24) which involves the value of V_{ε} and not its average. If we disregard this mathematical difficulty we obtain $D=\kappa+1$. So for random SE we have also $\eta=3-D$.

V. SERIES-PARALLEL BRANCHING

Since the SE has the same CPA as the Cantor-bar electrode introduced by Liu we now discuss the case of a tree as shown in Fig. 6. This geometry has essentially the same topology as the Cantor-bar electrode. In a lumped-circuit approximation the equivalent circuit of the tree is shown in Fig. 7(a). Here the series impedance $Z_{S,n}$ is the resistance of a square pore of length L_n and side a_n. The parallel impedance $Z_{P,n}$ is due to the capacitance of this pore:

$$Z_{S,n}=\rho L_n/a_n^2 , \tag{42}$$

$$Z_{P,n}=(4j\gamma\omega L_n a_n)^{-1} . \tag{43}$$

In the Cantor bar L_n is independent of the stage n, $L_n=L$. The impedance of the system of Fig. 6 is represented in Fig. 7(a). It can be written as a continued fraction

$$Z=Z_{S0}+\cfrac{1}{\cfrac{1}{Z_{P0}}+\cfrac{N}{Z_{S1}+\cfrac{1}{\cfrac{1}{Z_{P1}}+\cfrac{N}{Z_{S2}+\cfrac{1}{\cfrac{1}{Z_{P2}}+\cfrac{N}{Z_{S3}+\cdots}}}}}} \tag{44}$$

which is equal to

$$Z=Z_{S0}+\cfrac{1}{\cfrac{1}{Z_{P0}}+\cfrac{1}{\cfrac{Z_{S1}}{N}+\cfrac{1}{\cfrac{N}{Z_{P1}}+\cfrac{1}{\cfrac{Z_{S2}}{N^2}+\cfrac{1}{\cfrac{N^2}{Z_{P2}}+\cfrac{1}{\cfrac{Z_{S3}}{N^3}+\cdots}}}}}} \tag{45}$$

This is the continued fraction representing the impedance of circuit 7(b). So the tree is exactly equivalent to a "ladder" circuit. Those ladder circuits have been extensively studied by Oustaloup[28] and in many cases are known to present CPA behavior at high enough frequencies.

The ladder impedance can be calculated simply, in first approximation, using the following argument. One first remarks that if only the side a of the pore is divided by a factor α at each new branch, conserving L constant as in the Cantor-bar case, the ratio of the series impedance to the parallel impedance as a function of the stage goes as

$$Z_{S,n}/Z_{P,n}=4j\gamma\rho\omega L^2\alpha^n/a_0 \ . \tag{46}$$

At the first stage the series resistance is very small compared with the parallel resistance. But as one goes to smaller and smaller pores the ratio increases up to some critical stage ν where the ratio (46) is equal to 1. The index ν of this characteristic stage is given by

$$\omega=a_0/\alpha^{\nu}4\gamma\rho L^2 \ . \tag{47}$$

If α is large the series impedance corresponding to the stage $\nu+1$ is larger than $Z_{P,\nu}/\nu$ and can be considered as infinite in first approximation. In this situation the impedance is essentially that of stage ν because the series impedance before stage ν is small if α is large. Using (44) the value of the admittance is then in order of magnitude equal to

$$Y\sim N^{\nu}/2Z_{S,\nu}\sim(a_0^2/2\rho L)(a_0/4\gamma\rho L^2\omega)^{D-3} \ . \tag{48}$$

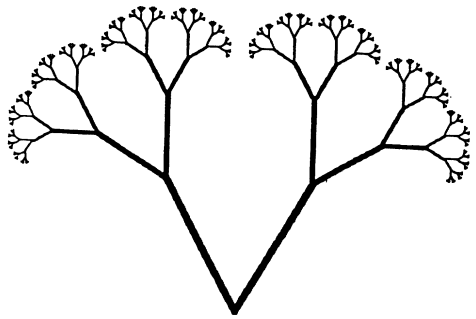

FIG. 6. Tree structure with the electrolyte in black. Each line represents a tube of side a_n and length L_n. In that structure the length is scaling as the side of the pore. On the contrary, the length is constant in the Cantor-bar case of Ref. 7.

This is essentially the same result that we obtained for the Sierpiński electrode. Although the geometry of the Cantor-bar electrodes could be regarded as basically different from the geometry of the modified finite Sierpiński electrodes they have the same properties. Here also the power is finally dissipated nonuniformly in the pores of characteristic frequency ω given by relation (47). It is not obvious that, following Liu, one can use an equivalent lumped circuit to describe the Cantor-bar impedance. This is, however, a good approximation because the larger pores behave indeed as resistors and capacitors. It is only the narrower pores which must be treated as lines. But these narrower pores are those whose series impedance is very large and play no role. The transition between these two approximations occurs when $\Lambda\sim L$, which just happens when the ratio (46) is equal to 1.

We think that this is a very important result because it tells us that whatever the branching—purely parallel in Sierpiński electrodes or series-parallel in the Cantor-bar electrode—the frequency dependence and the value of

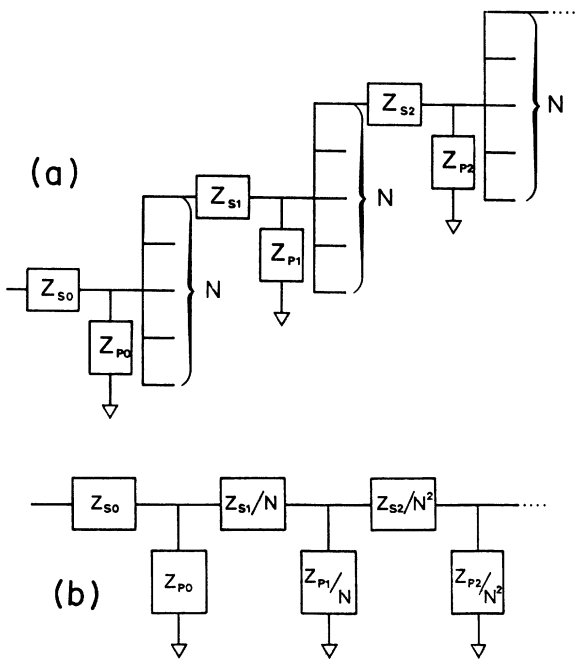

FIG. 7. Equivalent lumped circuits for trees. (a) Tree structure; (b) equivalent ladder structure.

the impedance are governed essentially by the number of characteristic pores at a given frequency.

If in the case of the tree the length itself scales as the side of the pores, then

$$Z_{S,n}/Z_{P,n}=4j\gamma\rho\omega L^2/a_0\alpha^n \tag{49}$$

and this ratio now decreases when n increases. The potential either penetrates the entire structure or does not penetrate at all and the response is not of the CPA type. This is an example where a true self-similar interface has not a CPA response.

Finally we consider a branched spherical-pore electrode (BSP) as shown in Fig. 8. This case is essentially equivalent to the above case of a tree. These electrodes are built with generators I or II also shown on the figure. Here each cavity of rank n gives access to N cavities of rank $n+1$, hence again we get N^n cavities of rank n. The ratio of the series to parallel impedance in the equivalent ladder is $Z_{S,n}/Z_{P,n}\sim(b_0/\Lambda)\alpha^{-n}$ and the signal does not penetrate the electrode if $\Lambda<b_0$ and goes to the smaller cavities if $\Lambda>b_0$. No CPA behavior is ever found. This seemingly comes from the fact that, in this model, the smaller the element, the shorter the characteristic R_nC_n associated time (in contrast to Liu's case). A more detailed study of the impedance shows that it can be written

$$Z_0=R_0+1/\{jC_0\omega+[-j/N^\mu C_\mu\omega+\mathcal{O}(NR_1)]^{-1}\}\ , \tag{50}$$

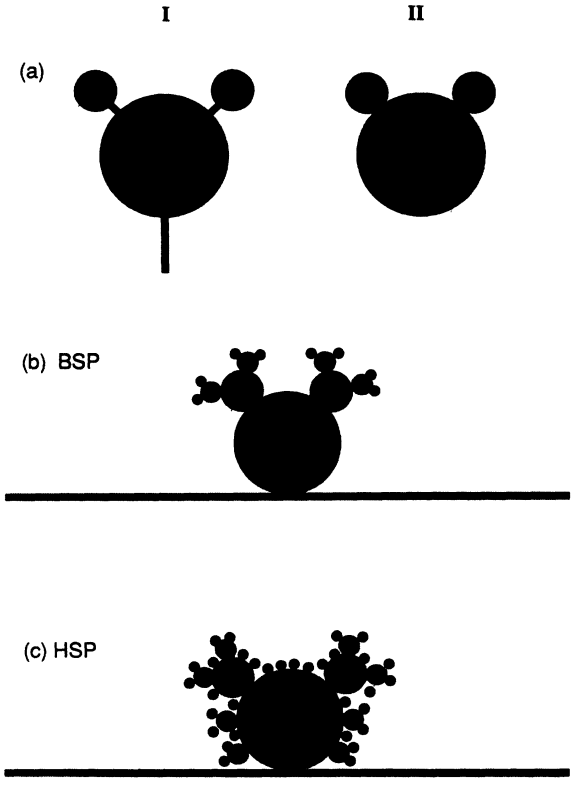

FIG. 8. Branched spherical-pore electrodes with the electrolyte in gray. (a) Generators I and II; (b) branched electrode (BSP); (c) hyperbranched electrode (HSP).

where $\mathcal{O}(NR_1)$ is a correction of order NR_1. As a consequence, no intermediate CPA regime can be present, even after subtraction of the series resistance R_0.

VI. HYPERBRANCHED SPHERICAL-PORE ELECTRODES AND POROUS ELECTRODES

The hyperbranched spherical pore electrode (HSP) is shown in Fig. 8(c). Here each cavity of rank n gives access to N cavities of rank $n+1$, N^2 cavities of rank $n+2$, $\ldots N^k$ cavities of rank $n+k,\ldots$, hence here we have $2^{n-1}N^n$ cavities of rank n. As discussed further this may be a good scheme for a part of a practical porous medium. A similar construction may be realized in two dimensions, and a cylinder may be built from this curve [hyperbranched cylindrical-pore electrode (HCP)]. Though it is of less physical relevance, this shape is interesting in that it bears similarity with shapes which have been considered by others, such as the Koch-island electrode or the related shapes of Ref. 14.

Of course, a constructibility problem can arise because it is not certain that one can build a mathematical fractal up to infinite decimation and keep the volume of the electrolyte finite. But we are concerned here by physical fractals which have a finite smaller scale and this question plays no role. So values of N and α outside the range of existence of the mathematical fractals of finite size may be considered. For practical objects the decimation will stop to a certain order μ, and, with an appropriate value for μ, these surfaces can be built for virtually any (N,α) doublets. The fractal dimensions, conditions of existence, and impedance behavior of these electrodes are summarized in Table I. In the following, we will only outline the derivation of the impedance behavior.

An equivalent circuit for the HSP electrode can be obtained by noticing that N identical series-parallel circuits (Z_S,Z_P) mounted in parallel may be represented as a single similar circuit $(Z_S/N,Z_P/N)$. (The same method has been used for the tree in Sec. V; see Fig. 7). The resulting circuit is shown in Fig. 9 (here represented for $\mu=4$). The impedance of this circuit is best obtained by starting from the right-hand side of the figure: calling Z_i the impedance as shown in the top of Fig. 9 (i.e., Z_i represents the impedance of N^i ith order cavities seen in parallel), examination of Fig. 9 makes a recursion relation appear:

$$Z_i=R_i/N^i+[jN^iC_i\omega+\sum_{k=i+1}^{\mu}Y_k]^{-1}\ \text{with}\ Y_k=1/Z_k\ . \tag{51}$$

This relation is schematized as the inset in Fig. 10. Figure 10 shows the results obtained after applying the recursion procedure for a HSP electrode with $N>\alpha,\alpha^2/2$. For such a case, the capacitance of the smallest cavities is dominant over that of the larger ones $[(2N)^nC_n>(2N)^{n-1}C_{n-1}$ since $N>\alpha^2/2]$. The recursion relation is applied starting from $Z_\mu=R_\mu/N^\mu-j/N^\mu C_\mu\omega$ and for decreasing values of i, from $\mu-1$ to 0. Except for unimportant deviations for the very first recursion steps, the results, shown graphically in Fig. 10, are that Z_i may be

TABLE I. Summary of the properties of various spherical-pore electrodes. PSP, parallel spherical pores; BSP, branched spherical pores; HSP, hyperbranched spherical pores; HCP, hyperbranched cylindrical pores. μ is the order of decimation of the smallest pores.

	Geometrical situation	Dimension D	Impedance behavior Z	η
PSP	$N<\alpha$	2	$(R_0-j/C_0\omega)$ (largest cavity dominant)	not CPA
	$\alpha<N<\alpha^2$	2	$R_0x(j\omega R_0C_0)^{-\eta}$	$\ln N/\ln\alpha-1$
	$N>\alpha^2$	$\ln N/\ln\alpha$	$(R_\mu-j/C_\mu\omega)N^{-\mu}$ (smallest cavities dominant)	not CPA
BSP	$N<\alpha^2$	2	$R_0-j/C_0\omega$	not CPA
	$N>\alpha^2$	$\ln N/\ln\alpha$	$R_0+[jC_0\omega+\mathcal{O}(1/R_1)]^{-1}$	not CPA
HSP	$N<\alpha^2/2$	2	$R_0-j/C_0\omega$	not CPA
	$\alpha^2/2<N<\alpha$	$\ln(2N)/\ln\alpha$	$R_0+[jC_0\omega+\mathcal{O}(1/R_1)]^{-1}$	not CPA
	$\alpha,\alpha^2/2<N$	$\ln(2N)/\ln\alpha$	$R_0\{1+[j\omega R_0(2N)^\mu C_\mu]^{-\eta}\}$	$\ln(N/\alpha)/\ln(2N/\alpha)$
HCP	$N<\alpha/2$	2	$R_0-j/C_0\omega$	not CPA
	$N>\alpha/2$	$1+\ln(2N)/\ln\alpha$	$R_0\{1+[j\omega R_0(2N)^\mu C_\mu]^{-\eta}\}$	$\ln N/\ln(2N)$

viewed as a large capacitance $(2N)^{\mu-i}C_\mu/2$ (i.e., it doubles each recursion step) in series with a resistance R_i/N^i, which increases each recursion step $(R_n/N^n>R_{n-1}/N^{n-1}$ since $N>\alpha)$. Graphical solution of the recursion relation shows that this simple RC character of Z_i is maintained down to Z_0. However, subtraction of the trivial series resistance R_0 makes the parallel branching of the Z_i's reappear, i.e., $(Z_0-R_0)^{-1}=jC_0\omega+Y_1+Y_2+\cdots+Y_\mu$. The impedance is made with the series resistance and capacitance of the larger pore and a parallel branching. This parallel branching straightforwardly leads to a CPA behavior $(Z_0-R_0)^{-1}\approx[j(2N)^\mu C_\mu R_0\omega]^\eta$ in the frequency range $\omega\gg(\rho\gamma b_0)^{-1}$ with an exponent

$$\eta=\ln(N/\alpha)/\ln(2N/\alpha) \tag{52}$$

as can be seen from inspection of Fig. 10. Other cases for N and α can also be considered. The results appear in Table I. So, for the HSP electrode a CPA behavior is obtained for a limited range of N and α. However, the CPA exponent is clearly unrelated to the fractal dimension. Furthermore, the borderline in the (N,α) plane for CPA behavior does not coincide with the fractal-nonfractal boundary.

Note that the geometry of a 2D Koch electrode (where the electrolyte enters the Koch "gulfs" such as considered in Ref. 14) belongs to the category of a HCP elec-

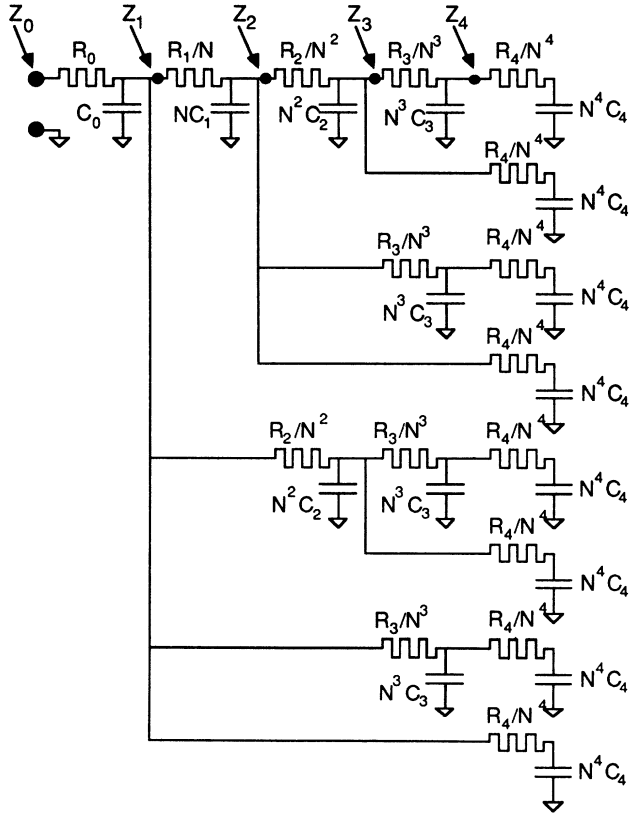

FIG. 9. Equivalent electrical circuit for HSP electrode. The impedance Z_i, obtained by taking a subcircuit at the right of each dot (see top of the figure) just corresponds to that of N^i pores of ith rank seen in parallel.

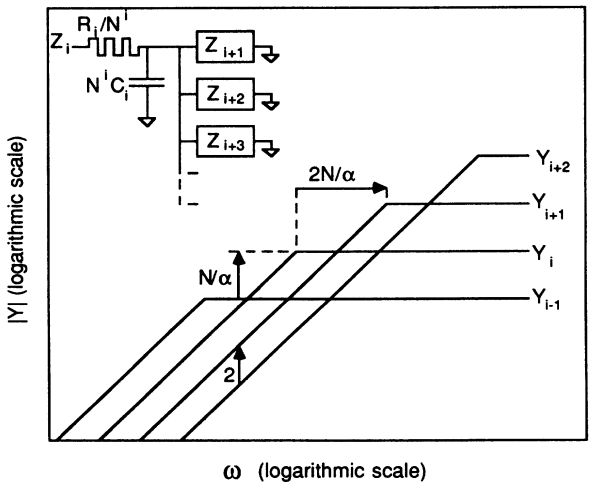

FIG. 10. Bode diagram study of HSP electrode. The inset illustrates the recursion relation [Eq. (51)].

trode. By this we mean that they are topologically equivalent. In that case the predicted exponent is $\ln N/\ln(2N)$ for the Koch profile, irrespective of the fractal dimension as in Ref. 14.

A most interesting point is that, here again, the impedance at a given frequency $\omega/2\pi$ is seen to arise from cavities of a given size $b_\nu = b_0\alpha^{-\nu}$, namely, from Z_ν such that

$$R_\nu N^{-\nu}(2N)^{\mu-\nu}C_\mu\omega \sim 1 ,$$

i.e.,

$$\nu \sim \ln[\rho\gamma b_0\omega(2N/\alpha^2)^\mu]/\ln(2N^2/\alpha) .$$

A noticeable point, however, is that Z_ν does not represent the impedance of *all* $(2N)^\nu/2$ cavities of size b_ν in the system, but only that of those N^ν such cavities which are accessed directly from the surface of the largest one. In other words, the cavities of size larger than b_ν will behave effectively as open switches and will prevent the ac potential excitation from reaching the smaller cavities branched on their walls, so that only the cavities smaller than b_ν *and* directly branched on the largest size cavity will participate to the impedance of the system.

These findings may tentatively be used to describe the behavior of a practical porous electrode. As suggested by Fig. 11, the HSP appears to provide a picture not too far from a realistic porous medium in that all sizes of cavities may be connected to the wall of a cavity of given size. A more general model would be one where a nth-rank cavity gives access to N_1 cavities of rank $n+1$, N_2 of rank $n+2,\ldots,$ N_k of rank $n+k,\ldots$. The HSP model corresponds to $N_k = N^k$, whereas the BSP corresponds to $N_1 = N$ and $N_k\ (k>1) = 0$.

A porous medium may be modeled, for example, by a piece of material where random spheres have been removed, say, K^n spheres of radius $b_n = b_0/\alpha^n$, located at random positions, for $n=0$ to μ. In such a model the average number of $(n+k)$th-rank cavities branched on a given nth rank cavity is $\sim K^{n+k}\alpha^{-3n-k} = (K/\alpha^3)^n(K/\alpha)^k$. This is just of the form N^k as for the HSP if $K=\alpha^3$, in which case $N=\alpha^2$, and $D = \ln(2\alpha^2)/\ln\alpha$, where $\eta = \ln\alpha/\ln(2\alpha)$ [in this special case we accidently get $\eta = 1/(D-1)\ldots$].

The impedance in the general case would, however, be more difficult to determine. Also, a realistic model should include randomness of the sizes of the cavities and connecting channels, and allow that a cavity inside the electrode be accessed from the surface through a nonmonotonic series of cavity sizes (i.e., large cavities might be accessed through smaller ones). We believe that the latter improvements would lead to exceedingly difficult calculations, but would not change the result significantly, especially in view of the above-demonstrated ability of a single large connecting cavity for generating a dead end at the higher frequencies. A plausible model for a practical porous electrode therefore appears as a flat surface with various HSP's branched in parallel (e.g., 1 HSP of largest size index 0, N HSP's of index 1, . . . , and N^n HSP's of index $n,\ldots$). As we have seen, a single HSP just behaves like an RC circuit if the series resistance is not subtracted. It then presents a Bode diagram with a "shoulder" and a parallel branching of such circuits will give rise to CPA. The impedance of such an electrode is just $R_0(j\omega/\omega_0)^\eta$, with $\omega_0 = [R_0C_\mu(2N)^\mu/2]^{-1}$ and $\eta = \ln(N/\alpha)/\ln(2N/\alpha)$, in the range $\omega_0 \ll \omega \ll 1/R_\mu C_\mu$, and for $N > \alpha, \alpha^2/2$, whereas its fractal dimension is $\ln(2N)/\ln\alpha$.

In conclusion, these various examples confirm the view, already emerging from the Sierpiński electrodes, that the CPA regime and exponent for a blocking electrode have little to do with its fractal dimension and even with its fractal nature. Rather, a most important point seems to be whether the scaling elements are mounted in series or in parallel. Parallel elements will easily lead to CPA behavior, whereas serial elements can only do so if the characteristic time constant of the element increases with decreasing element size (e.g., the Liu electrode). The example of the HSP electrode is instructive in this respect, as it involves parallel and serial character at the same time, and it appears clearly in the course of the evaluation of the impedance that the exponent essentially arises from the parallel mounting of the Z_n's.

Figure 12 shows the accessible pores of a porous electrode of the type shown in Fig. 11. At a given frequency all these pores are not equally active. Only those which are accessed through pores of size $\leq b_\nu$ play a role at that frequency. This is to be related to the known fact that in practical porous electrodes only a small part of the surface is really active.

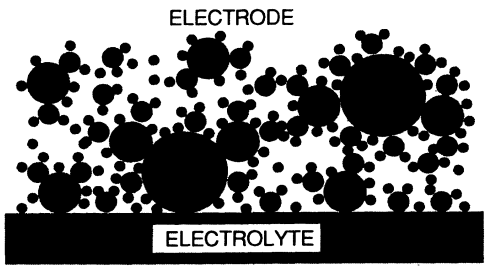

FIG. 11. A quasiporous system build from superposition of hyperbranched spherical pores. All the pores are active in the diffusion regimes described in Sec. IX.

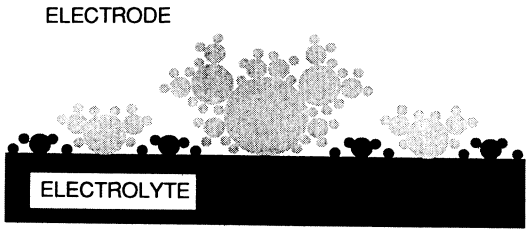

FIG. 12. Possibly active pores of a porous electrode in the blocking or nonblocking regime with no diffusion. This is equivalent to the electrode of Fig. 11 where buried pockets are inactive at all frequencies. Active pores at a given frequency are shown by hatching. Only the regions connected to the external surface through spheroids of size $\leq b_\nu$ are active at a given frequency. The critical size b_ν of the "entry" is proportional to $\omega^{-\ln\alpha/(\ln 2 + 2\ln N - \ln\alpha)}$.

VII. dc FARADAIC RESPONSE AND ROLE OF THE INTRINSIC SURFACE PROPERTIES

We can deduce the dc response from the ac response if we use the fact that the response is an holomorphic function of the variable $r+(j\gamma\omega)^{-1}$ as we have discussed in Sec. IV. In order to obtain the response we have only to replace $j\gamma\omega$ by r^{-1} in Eq. (21) and

$$Y_{dc}\sim(La_0/r)(a_0r/L^2\rho)^{1-\eta}\ . \tag{53}$$

One can verify easily that the admittance of a fractal system is enhanced by the fractal geometry as compared to the admittance of a single pore of side a_0. The most interesting comment on Eq. (53) arises from the power dependence of the admittance as a function of r and ρ. The admittance is proportional to $r^{-\eta}$. This result, although it is obtained in a somewhat trivial geometry, is not trivial. It means, for instance, that dividing the surface resistance at the very surface of a porous electrode by a factor of 2 will not double the current. The current is not proportional to the electrolyte conductivity but rather to $\rho^{\eta-1}$. As a consequence, the macroscopic coefficient of response across a fractal interface is not proportional to the microscopic transport coefficients. A power law depending on the hierarchy relates these factors. This conclusion could have applications in several systems found in nature or built to have large surface porous structures. One should also note that none of these responses are proportional to the square of the size of the object. Although one has neglected the resistance of the small electrolyte layer between the two electrodes, there exists an effective finite real admittance Y_{FR} in series with the CPA element.

The same type of discussion applies to the different geometries considered above: It shows that in general, apart from diffusion effects, a number of electrodes, fractal or nonfractal, may exhibit an impedance of the form

$$Z\propto R_{el}+[Y_{dc}+k(j\omega)^{\eta}]^{-1}\ . \tag{54}$$

This is the form that was empirically introduced to describe rough or porous electrodes [1,3] but the purely dc part of it $(R_{el}+Y_{dc}^{-1})$ is also geometry dependent in a nontrivial way. This conclusion could have applications in several systems found in nature or built to have large surface porous structures.

The same kind of argument permits us to predict the response of a SE in the case where the surface itself has an intrinsic response of the form $(j\omega)^{\chi}$ even for a planar surface. This is often the case practically and can be qualitatively attributed to random microscopic transport near the interface. In that situation the response should have the form $Y\sim(j\omega)^{\chi\eta}$. This permits one to understand quantitatively the experimental results of Keddam and Takenouti who measure $\chi=0.89$ and $\eta=0.5$.[20]

The same argument might be taken to conclude that an exponent $\eta/2$ will be found in the presence of a diffusion impedance. We could consider that the surface itself has a specific admittance of the form $j\gamma\omega+(r+Z_{\mathcal{D}})^{-1}$. The admittance of the electrode being an holomorphic function of ω we would find the diffusive response by replacing $\gamma\omega$ by $(Z_{\mathcal{D}})^{-1}\propto(j\omega)^{1/2}$ in the diffusive regime and obtain an exponent $\eta/2$. We will however see in Sec. IX that further complications arise at low frequencies so that this result is not general. The reason is that when the diffusion length is too large one cannot consider a surface admittance for a fractal surface.

VIII. EDGE EFFECTS

Most of the above examples (i.e., the various Sierpiński electrodes or the Liu electrode) involved pores, which were treated in the de Levie approximation, that is, as one-dimensional lossy lines. This approximation is valid in the regime where the penetration depth $\lambda_n=(a_n/4\rho\gamma\omega)^{1/2}=(a_n\Lambda/4)^{1/2}$ is much larger than the lateral dimension of the pore a_n. At frequencies $\omega\geq 1/(4\rho\gamma a_n)$ this condition is violated and the map of the current lines across the pore has to be considered in more detail. Here, we will study these edge effects and examine the modifications that they imply on the above results.

Let us reconsider the case of a single pore at a very high frequency $[\omega\gg 1/(4\rho\gamma a_n)]$. As was assumed in Sec. II, we take the counter electrode in the plane of the opening of the pore, and the front surface of the electrode is isolated (e.g., by an insulating varnish). Since the frequency is very high, the capacitance of the pore walls acts almost as a short circuit, and the current lines are concentrated near the edges of the opening. Then for convenience this opening may as well be simulated by a rectilinear corner of length $4a_n$ (see Fig. 13). At very high frequency the pore wall may be considered as a short circuit, the potential in the vicinity of the wall $[\lim_{y\to 0+}V(x,y)]$ is constant, hence the current lines end normally to the wall except very near the corner as shown below. From the Poisson equation, it then follows that the current lines are simply quadrants centered at the edge. The current lines ending between x and $x+dx$ carry the current $V/(\rho\pi x/8a_n dx)$, hence the total current is

$$I=V(8a_n/\pi\rho)\int_{x_1}^{x_2}x^{-1}dx\ . \tag{55}$$

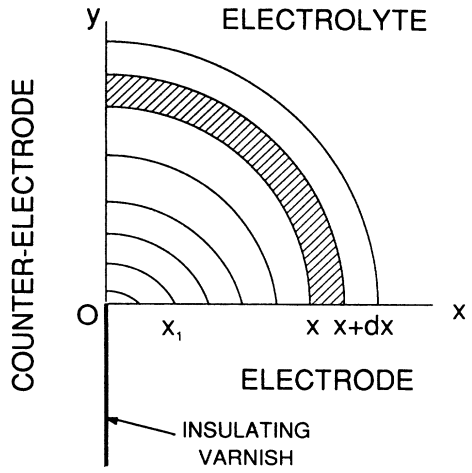

FIG. 13. Electric field lines in the very high-frequency regime in which edge effects are dominant.

The higher integration bound x_2 should obviously be taken as a cutoff length of order a. The lower integration bound x_1 is given by the point where the short-circuit approximation for the wall capacitance ceases to be valid. This occurs when the conductance of the channel ending between x_1 and x_1+dx is of the same order of magnitude as the associated wall susceptance, that is,

$$(1/\rho)(8a_n dx/\pi x_1)\sim\gamma 4a_n\omega dx\ , \tag{56}$$

hence $x_1\sim\Lambda$ and

$$Y=I/V\approx(8a_n/\pi\rho)\ln(a_n/\Lambda)\ . \tag{57}$$

The x values smaller than x_1 actually bring also a contribution to Y, of the order of $j\gamma\omega 4a_n x_1\sim 4ja_n/\rho$. This, however, does not change the order of magnitude of the admittance. It is seen from Eq. (57) that the admittance is of the order of a_n/ρ and depends only weakly upon the frequency. This may be understood intuitively: a series resistance of order ρ/a_n (i.e., a cube of dimension a_n) is the minimum price that the current has to pay for entering the pore. The logarithmic dependence of Y upon ω exhibited by Eq. (57) is somewhat embarrassing for the following, though it does not bring anything to the results. Moreover, it is probably unphysical, as it arises from the very peculiar geometry that we have taken for the counter electrode. For these reasons, we will rather take for the edge-limited admittance a constant value $Y_{\max}=\xi a_n/\rho$, where ξ is a dimensionless constant of the order of a few units. The resulting admittance of a single pore as a function of ω now exhibits three regions, sketched in Fig. 14(a). The central $\omega^{1/2}$ regime will survive provided the pore is long ($L_n\gg a_n$). We will now examine the consequences of these edge effects upon the admittance of the Sierpiński and Cantor bar electrodes.

Figure 14(b) shows the various parallel contributions to the admittance that will occur for a Sierpiński electrode. The largest pore (a_0,L) will give the dominant contribution in the $\omega^{1/2}$ region $(a_0/4\rho\gamma L_0^2\ll\omega\ll\xi^2/4\rho\gamma a_0)$. For smaller pores, however, the $\omega^{1/2}$ region will extend to lower frequencies (the crossover frequency from ω to $\omega^{1/2}$ scales as a_n/L_n^2, hence decreases with decreasing pore size), but also to higher frequencies (the crossover frequency from $\omega^{1/2}$ to ω^0 scales as $1/a_n$, hence increases with decreasing pore size). As seen in Fig. 15, the contribution of the smaller pores may become dominant as well for $\omega\gg\xi^2/4\rho\gamma a_0$ as for $\omega\ll a_0/4\rho\gamma L_0^2$. In the lower frequency range, the total admittance will be ruled by the exponent η calculated in Sec. II. A new exponent η' will appear in the higher frequency range $\omega\gg\xi^2/4\rho\gamma a_0$. It is given by $\eta'=\ln(N/\alpha)/\ln\alpha=(\ln N/\ln\alpha)-1$. For the

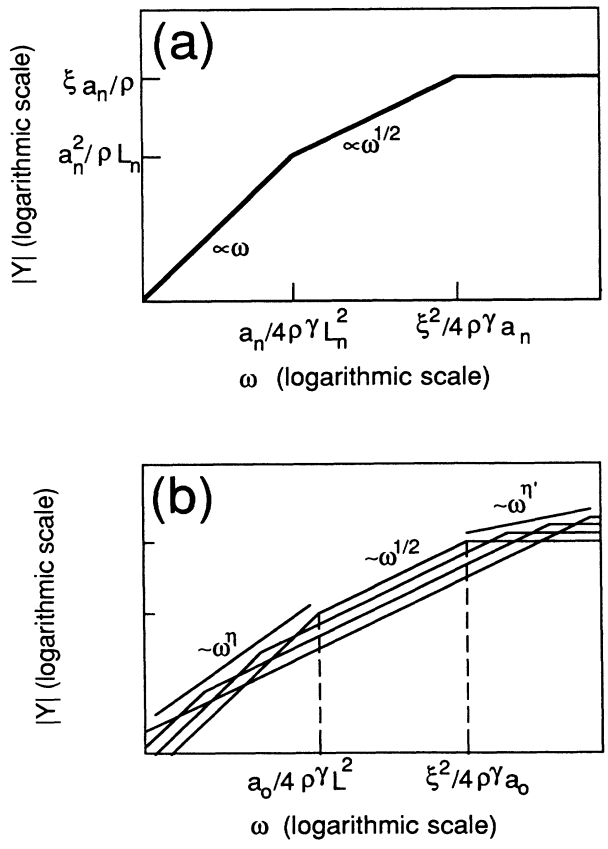

FIG. 14. (a) Bode diagram of a single square pore when edge effects are taken into account. (b) Bode diagram study of the generalized Sierpiński electrode in the presence of edge effects.

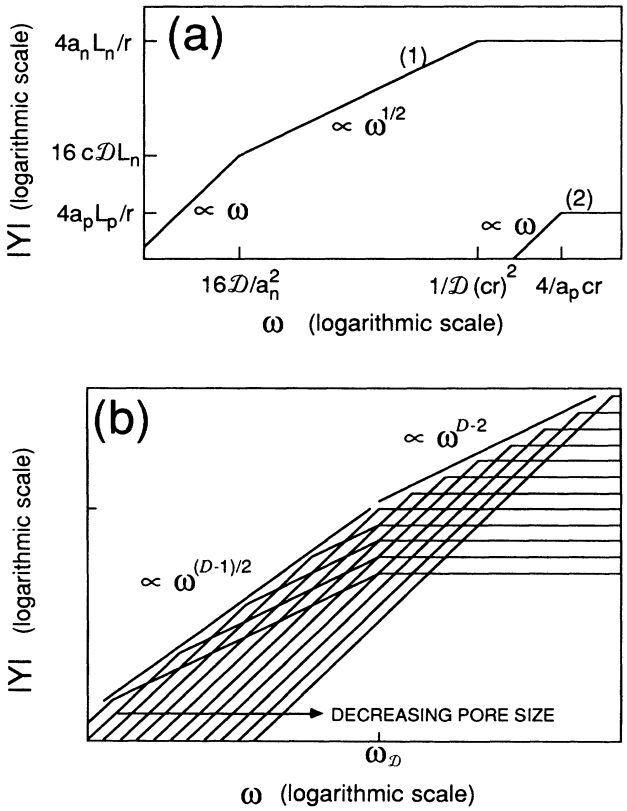

FIG. 15 (a) Bode diagram of a square pore in a system with only diffusion and Faradaic resistance. Curves (1) and (2) correspond, respectively, to a large pore and a small pore ($n<p$). (b) Bode diagram of the generalized Sierpiński electrode in the diffusion plus Faradaic resistance regime. The two exponents are directly related to the fractal dimension.

generalized SE one has $0<\eta'<1/2$ in the allowed range for (N,α,α_z). In the special case $\alpha_z=1$ it gives $\eta'=D-2=1-\eta$ but in general it cannot be a function of D as it is independent of α_z.

For the case of the Cantor-bar electrode, the pores are in series and it turns out that the edge limitation has no effect on the result. No CPA behavior due to edge effects will exist in this case.

In summary, it appears that edge effects may introduce new frequency domains where the admittance will follow a CPA behavior with a specific exponent. It is not clear, however, that the above exponent η' for the Sierpiński electrode will be observable in practice: for example it is doubtful that the front surface of a practical electrode can be insulated, and the $\omega^{\eta'}$ behavior can be partially masked by the shunting capacitance of the front surface. The possible existence of edge-ruled regimes should not, however, be overlooked in general, especially in the case of electrodes made of needles instead of pores.

IX. DIFFUSION EFFECTS

In Sec. VII we have considered the effect of a Faradaic resistance in parallel with the interface capacitance. However, we have not taken yet diffusion effects into account. We recall that an electrochemical reaction ("Faradaic process") may become diffusion limited whenever "indifferent" charged species (i.e., nonparticipating to the electrochemical reaction) are present in the electrolyte simultaneously as the "electroactive" participating species. If a large concentration of indifferent species exists and a small potential step is applied, the interface capacitance will be charged after a short time because the solution is sufficiently conductive and the applied potential will then appear across the interface. A large initial Faradaic current will then flow, but this will change the concentrations of the electroactive species in the vicinity of the interface. If the transfer kinetics is not rate limiting, the surface concentrations will be imposed by the value of the potential. Since the solution is highly conductive, no electric field will be left and the only driving force for bringing new electroactive species to the interface will be the concentration gradient, through a diffusion process. To calculate the diffusion impedance $Z_{\mathcal{D}}$ one considers small concentrations $c_{\rm red}$ and $c_{\rm ox}$ of the species "red" and "ox" which participate in the electrochemical reaction: reducing agent red$\rightarrow$oxidized agent ox$+ze^-$. For convenience, we will assume that both the reducing and oxidized agents have the same diffusion constant $\mathcal{D}$. When a planar electrode is submitted to a small applied potential $\mathrm{Re}(Ve^{j\omega t})$ $(V\ll kT/e)$ the surface concentrations will become $c_{\rm red}-\delta c_0$ and $c_{\rm ox}+\delta c_0$, with

$$\begin{aligned} V&=(kT/ze)\{\ln[(c_{\rm ox}+\delta c_0)/(c_{\rm red}-\delta c_0)] \\ &\qquad -\ln(c_{\rm ox}/c_{\rm red})\}\ , \\ V&\approx(kT/ze)\delta c_0(c_{\rm ox}^{-1}+c_{\rm red}^{-1})\ , \end{aligned} \tag{58}$$

and the concentration profile $\delta c(x)$ will be ruled by the diffusion equation

$$j\omega\,\delta c=\mathcal{D}\,\partial^2\delta c/\partial x^2\ , \tag{59}$$

hence

$$\delta c(x)=\delta c_0\exp(-x/\Lambda_{\mathcal{D}}) \quad \text{with } \Lambda_{\mathcal{D}}=(\mathcal{D}/j\omega)^{1/2}\ . \tag{60}$$

The electrochemical current will be

$$J=-ze\mathcal{D}(\partial\delta c/\partial x)_{x=0}=ze(j\omega\mathcal{D})^{1/2}\delta c_0\ . \tag{61}$$

Physically, this means that the charge passed through the interface during a cycle corresponds to a number of species in a concentration δc_0 contained in the diffusion layer of thickness $\Lambda_{\mathcal{D}}\sim(\mathcal{D}/\omega)^{1/2}$. The associated admittance for an electrode area S is

$$\begin{aligned} Y_{\mathcal{D}}=Z_{\mathcal{D}}^{-1}&=JS/V \\ &=S(z^2e^2/kT)[c_{\rm ox}c_{\rm red}/(c_{\rm red}+c_{\rm ox})](j\omega\mathcal{D})^{1/2} \end{aligned} \tag{62}$$

and defining

$$c=(z^2e^2/kT)c_{\rm red}c_{\rm ox}/(c_{\rm red}+c_{\rm ox})\ , \tag{63}$$

$$Y_{\mathcal{D}}=Z_{\mathcal{D}}^{-1}=Sc(j\omega D)^{1/2}\ . \tag{64}$$

The quantity c is a capacitance per unit volume; we call it specific diffusive capacitance. Then in the case of a sinusoidal perturbation, one will find the so-called Warburg impedance behavior $Z_{\mathcal{D}}\propto(j\omega)^{-1/2}$ for a flat surface.[29] It is interesting to write Eq. (64) in the following form:

$$|Y_{\mathcal{D}}|=S(\mathcal{D}/\omega)^{1/2}c\omega \tag{65}$$

because it tells us that the diffusive admittance is simply that of the capacitance of the diffusive volume. We show below that this can be extended to fractal surfaces.

The case of a diffusion-limited process at a fractal electrode has been considered by Nyikos and Pajkossy for the Koch-island electrode.[22] We will first show that their result also holds true for Sierpiński electrodes and is, in fact, quite general. We will see that the diffusive response of a fractal electrode is directly related to the exterior Minkowski-Bouligand dimension. The notion of a Minkowski-Bouligand neighboring is shown to apply very generally to any surface, fractal or not. Then, we will consider the changes that occur when the Faradaic resistance and electrolyte resistance are not neglected. Finally, we will incorporate the interface capacitance and deduce a typical behavior for a practical Sierpiński electrode.

A. Diffusion alone

Equation (65) states that the charge passed through the interface during a cycle corresponds to the diffusive capacitance contained in the diffusion layer of thickness $\sim(\mathcal{D}/\omega)^{1/2}$. If the electrode is now a pore of length L_n and edge a_n, at high enough frequencies $(\omega\gg\mathcal{D}/a_n^2)$ the diffusion depth $(\mathcal{D}/\omega)^{1/2}$ will be much smaller than a_n and the admittance will be

$$Y_{\rm HF}=c(j\omega\mathcal{D})^{1/2}\times 4a_nL_n\ . \tag{66}$$

In the opposite limit $\omega \ll \mathcal{D}/a_n^2$, the equilibrium concentration will be reached at any time in all the volume of the pore, hence the current passed through the interface will correspond to a concentration δc_0 in the volume $a_n^2 L_n$; hence

$$I_{\mathrm{LF}} = zej\omega\, \delta c_0\, a_n^2 L_n \ , \tag{67}$$

$$Y_{\mathrm{LF}} = cj\omega a_n^2 L_n \ . \tag{68}$$

The diffusion admittance for a pore is therefore qualitatively similar with the admittance considered in Sec. II (an ω regime followed by a $\omega^{1/2}$ regime), but here the scaling behavior of the crossover point is given by $\omega_n \propto 1/a_n^2$ and $|Y_{c,n}| \propto L_n$. When a generalized Sierpiński electrode is considered, this gives an exponent

$$\eta_{\mathcal{D}} = \ln(N/\alpha_z)/2\ln\alpha = (D-1)/2$$

using Eq. (26). This result is the same as that found by Nyikos and Pajkossy for a Koch-island electrode. We are going to show here that this agreement is not fortuitous and that $\eta_{\mathcal{D}} = (D-1)/2$ is a general result for the diffusion admittance at a fractal electrode.

The general form of the diffusion admittance at a fractal electrode can be found by considering the number of species $\nu(\omega)$, in a concentration δc_0, contained in the vicinity of the electrode surface up to a distance of the order of $\Lambda_{\mathcal{D}} \sim (\mathcal{D}/\omega)^{1/2}$. The admittance is then $|Y| \sim \nu(\omega)(ze\omega/V)$. Now, according to the exterior Minkowski-Bouligand fractal dimension, the volume located within a distance $\Lambda_{\mathcal{D}}$ from the fractal varies as $\Lambda_{\mathcal{D}}^{3-D}$, hence $\nu(\omega) \propto \Omega((\mathcal{D}/\omega)^{1/2}) \propto \omega^{(D-3)/2}$ and $|Y(\omega)| \propto \omega^{(D-1)/2}$. More precisely, if a fractal electrode has a macroscopic surface S the content of the neighboring $\Omega(\Lambda_{\mathcal{D}})$ is equal to $S^{D/2}\Lambda_{\mathcal{D}}^{3-D}$ and using Eq. (65) with this diffusive volume, one obtains

$$|Y_{\mathcal{D}}| = S^{D/2}\mathcal{D}^{(3-D)/2} c\omega^{(D-1)/2} \ . \tag{69}$$

Here again, there is an anomalous power-law behavior related to the fractal geometry. In the limit $D=2$ one obtains the usual diffusion admittance of Eq. (64). One should emphasize that this reasoning is general: for any surface a volume $\Omega(\Lambda_{\mathcal{D}}) = \Omega((\mathcal{D}/\omega)^{1/2})$ exists and the admittance is

$$|Y_{\mathcal{D}}| = c\omega\Omega(\mathcal{D}/\omega)^{1/2} \ . \tag{70}$$

This relation provides the principle of a new kind of measurement of surface roughness. It is usable for any kind of surface at the condition that diffusion is the limiting step to the electrochemical transfer. We will now consider what happens when the Faradaic resistance and series resistance of the electrolyte are non-negligible. We will mostly restrict this discussion to the case of Sierpiński electrodes.

B. Diffusion and Faradaic resistance

At high enough frequencies, the diffusion admittance of a planar electrode becomes larger than the Faradaic admittance itself, and the overall admittance then stays constant upon further increase of ω. The crossover between the two regimes occurs at a frequency $\omega_{\mathcal{D}} = 1/\mathcal{D}(cr)^2$ obtained by equating Eq. (64) to Sr^{-1}.

In the case of a pore of a generalized SE, two kinds of behavior may occur depending upon whether this crossover appears above or below the ω to $\omega^{1/2}$ crossover frequency quoted above. These two cases are represented in Fig. 15(a). If $a_n \gg 4\mathcal{D}cr$, one will find the ω regime at the lowest frequencies, followed by the $\omega^{1/2}$ regime above $\omega \sim 16\mathcal{D}/a_n^2$, itself followed by the ω^0 regime above $\omega_{\mathcal{D}}$. If $a_n \ll 4\mathcal{D}cr$ the ω regime will directly turn to the ω^0 regime above $\omega \sim 4/a_n cr$. When a generalized SE is considered, Fig. 15(b) shows that two regimes may be obtained. The ω to $\omega^{1/2}$ crossover point scales as $\omega \propto 1/a_n^2$, $|Y| \propto L_n$, hence the exponent $\eta_{\mathcal{D}} = \ln(N/\alpha_z)/2\ln\alpha = (D-1)/2$, already found in the diffusion-only case. This regime, however, will stop at the higher frequencies $\omega > \omega_{\mathcal{D}}$ and it will be followed by a regime determined by the smallest pores, for which the admittance turns directly from ω to ω^0. The scaling of this crossover point ($\omega \propto 1/a_n, |Y| \propto a_n L_n$) then yields a new exponent

$$\eta'_{\mathcal{D}} = \ln(N/\alpha\alpha_z)/\ln\alpha = D-2 \ , \tag{71}$$

valid whatever the value of D between 2 and 3.

This exponent again seems to be quite universal. Its validity can be verified, e.g., for the spherical-pore electrodes considered above whatever their structure. This may be understood intuitively as follows: because the electrolyte is equipotential, a small electrolyte pocket of size b acts as an effective capacitance of order cb^3 in series with a Faradaic resistance of order r/b^2. Hence the BD of a pocket of size b_n has a characteristic frequency ω_n of order crb_n^{-1}. As the frequency is increased, smaller pockets are being probed. At a frequency ω the behavior will be governed by the pores of size Λ'

$$\Lambda' = (rc\omega)^{-1} \ , \tag{72}$$

which, in a fractal surface of macroscopic size S, are in number $n(\Lambda')$

$$n(\Lambda') = S^{D/2}(\Lambda')^{-D} \ . \tag{73}$$

We have then a parallel connection (because the volume is equipotential) of $n(\Lambda')$ circuits of admittance $(\Lambda')^2 r^{-1}$ and the admittance of the electrode is

$$Y = n(\Lambda')(\Lambda')^2 r^{-1} = S^{D/2} r^{-1} (rc\omega)^{D-2} \ . \tag{74}$$

The change of behavior from $\omega^{\eta_{\mathcal{D}}}$ to $\omega^{\eta'_{\mathcal{D}}}$ will occur for $\omega_{\mathcal{D}} \sim 1/\mathcal{D}(cr)^2$. For typical values ($\mathcal{D} \sim 10^{-5}$ cm^2/s, $c \sim 10^2$ F/cm^3, $r \sim 10\ \Omega\,\mathrm{cm}^2$) this gives $\omega_{\mathcal{D}} \sim 10^{-1}\ \mathrm{s}^{-1}$ and the critical pore size $a_n \sim 4\mathcal{D}cr$ is ~ 0.1 mm. This seems to indicate that the diffusion-only regime ($\eta_{\mathcal{D}} = (D-1)/2$) will hardly be observed except at very low frequencies or for systems with a very small value of r.

Note that when $D=2$ the admittance is Sr^{-1} as expected in the Faradaic regime for a planar electrode. Here again the admittance presents power-law dependences as a function of the physical parameters of the system r, c, S, and ω. The same kind of approach can be applied to any kind of surface, fractal or not, as long as it is made of relatively closed pockets.

The very general reason for which one can relate these regimes to the fractal dimension is that, due to the presence of the support electrolyte, the volume of the electrolyte is electrically equipotential. The electrochemical potential is nonuniform on a scale of the order of the diffusion length. The cause for this nonuniformity is the electrical potential drop at the exchange surface. Since the electrical potential is uniform, this excitation is constant over the surface. As a consequence, the perturbation occurs only very near the surface and the flux at some point on the surface is a local response. The ionic diffusion mechanism itself always takes place in the Euclidian space occupied by the electrolyte and is not perturbed by the presence of the fractal surface which acts only as a boundary. It is therefore not surprising that this flux can be related to some dimension through a "fattening" of the surface as done in the Minkowski-Bouligand approach.

On the contrary, if the resistance of the electrolyte plays a role, the electrolyte is no more equipotential and the response is no more local. In that case the admittance is not related to the local properties of the interface as characterized through the fractal dimension.

C. Taking the series resistance of the electrolyte into account

The derivation, given in Sec. II, of the potential distribution along a pore in the de Levie approximation, can be revisited for an interface admittance more general than the simple r,γ model of Sec. II. In general, for a planar interface, the admittance will be dominated by diffusion at low frequencies, and by the interface capacitance at high frequencies; a plateau may possibly appear at intermediate frequencies due to the Faradaic resistance, as shown in Fig. 2. In the case of a pore, the diffusion regime will further exhibit the ω regime at the lowest frequencies, as explained above. Calling $1/\zeta(\omega)$ the interface admittance per unit interface area of the pore wall (sketched in Fig. 16) de Levie's calculation still holds true, provided that $(j\gamma\omega+r^{-1})$ is replaced by $1/\zeta(\omega)$. This is not completely obvious in the lowest frequency regime ($\omega \ll \mathcal{D}/a_n^2$) as diffusion along the pore might affect the result. However, one can check that this effect is negligible in the case where the electroactive species are in a concentration much smaller than that of the indifferent species.

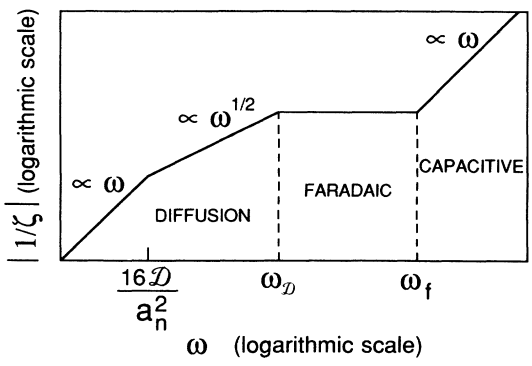

FIG. 16. Bode diagram of the "equivalent" admittance of the surface of a pore including the diffusive low-frequency regimes.

It is then found that the potential modulation penetrates into the pore to a characteristic depth $\Lambda_n \sim(4\rho/|\zeta|a_n)^{-1/2}$, i.e.,

$$V(x)=-(\rho\Lambda_n/a_n^2)I(x)\cosh(x/\Lambda_n)\,, \tag{75}$$

$$Y=(a_n^2/\rho\Lambda_n)\tanh(L_n/\Lambda_n)\,. \tag{76}$$

Since $|\zeta|$ is a monotonically increasing function of ω, the penetration length Λ_n decreases with increasing frequency. For frequencies below a critical ω_c, one will then have $\Lambda_n \gg L_n$, hence $Y\sim a_n^2L_n/\rho\Lambda_n^2=4a_nL_n/\zeta$ (the series resistance of the electrolyte is negligible). For frequencies larger than ω_c, then $\Lambda_n \ll L_n$ and

$$Y\sim a_n^2/\rho\Lambda_n=[(a_n^2/\rho L_n)(4a_nL_n/\zeta)]^{1/2}\,.$$

In other words, the admittance is the geometric mean of the interface admittance and the series conductance of the channel.

We will first limit the discussion to the joint effects of diffusion and electrolyte resistivity. The admittance of a single pore is shown in Fig. 17(a). Two cases may be en-

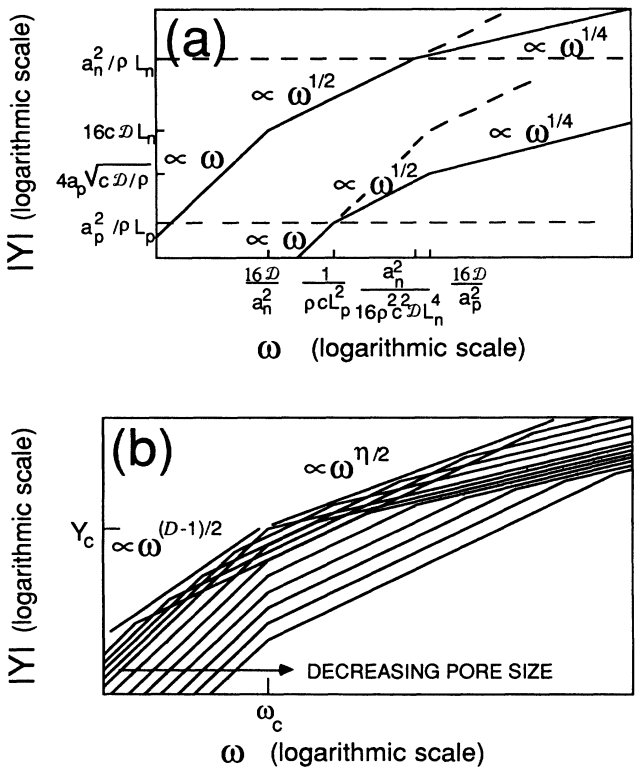

FIG. 17. (a) Bode diagram of the admittance of one pore in the diffusive plus electrolyte resistivity regime (low-frequency part). Two cases are shown, depending upon the pore size ($n<p$). (b) Bode diagram of the generalized Sierpiński electrode in the diffusive plus electrolyte resistivity regime (low-frequency part). The low-frequency exponent depends directly on the fractal dimension whereas, at higher frequencies, a different exponent appears. This last exponent is not related to the fractal dimension.

countered. If $a_n^2/L_n^2 \gg 16\rho c\mathcal{D}$ three regions will be found: ω at the lowest frequencies, then $\omega^{1/2}$ for $\omega > 16\mathcal{D}/a_n^2$, then $\omega^{1/4}$ for $\omega > a_n^2/16\rho^2c^2\mathcal{D}L_n^4$. If $a_n^2/L_n^2 \ll 16\rho c\mathcal{D}$ three similar regimes will be found, but the crossover frequencies will be $1/\rho cL_n^2$ (for the ω to $\omega^{1/2}$ crossover) and $16\mathcal{D}/a_n^2$ (now for the $\omega^{1/2}$ to $\omega^{1/4}$ crossover).

The resulting behavior for the Sierpiński electrode can be seen in Fig. 17(b). The situation is made somewhat complex by the crossing of the two crossover frequencies upon varying pore size. A critical pore size occurs for $a_{nc}^2/L_{nc}^2 \sim 16\rho c\mathcal{D}$, which means

$$n_c \sim \ln(a_0^2/16\rho c\mathcal{D}L_0^2)/\ln(\alpha/\alpha_z) .$$

We will call ω_c the associated frequency ($\omega_c = 16\mathcal{D}/a_{nc}^2 = 1/\rho cL_{nc}^2 = [(16\mathcal{D}/a_0^2)^{\ln\alpha} \times (\rho cL_0^2)^{\ln\alpha_z}]^{1/\ln(\alpha/\alpha_z)}$) and Y_c the contribution of those pores. The pores larger than the critical size ($a_n/L_n \gg a_{nc}/L_{nc}$) yield an admittance behavior $|Y| \sim |Y_c|(\omega/\omega_c)^{\eta_{\mathcal{D}}}$ for $\omega \ll \omega_c$ and $|Y| \sim |Y_c|(\omega/\omega_c)^{\eta_{\mathcal{D}S}}$ for $\omega \gg \omega_c$ with $\eta_{\mathcal{D}} = \ln(N/\alpha_z)/2\ln\alpha = (D-1)/2$ and $\eta_{\mathcal{D}S} = \ln(N\alpha_z/\alpha^2)/2\ln(\alpha_z^2/\alpha)$, which is not a function of D (actually $\eta_{\mathcal{D}S} = \eta/2$, which lies between $\frac{1}{4}$ and $\frac{1}{2}$). The pores smaller than the critical size ($a_n/L_n \ll a_{nc}/L_{nc}$) yield a behavior $|Y| \sim |Y_c|(\omega/\omega_c)$ for $\omega \ll \omega_c$, which is negligibly small compared to the contribution of the larger pores. For $\omega \gg \omega_c$, the higher crossover point follows a line with slope $\ln(N/\alpha)/2\ln\alpha$. However, for the allowed range of N and α, this quantity is smaller than $\frac{1}{4}$, hence this contribution is negligible.

In conclusion, one finds the diffusion-only exponent $\eta_{\mathcal{D}} = (D-1)/2$ for $\omega \ll \omega_c$, and a regime $|Y| \propto \omega^{\eta_{\mathcal{D}S}}$ for $\omega \gg \omega_c$, with $\eta_{\mathcal{D}S} = \eta/2 = \ln(N\alpha_z/\alpha^2)/2\ln(\alpha_z^2/\alpha)$. This exponent $\eta/2$ was indeed expected from our discussion of Sec. VII. The contribution of the larger pores [$a_n/L_n \gg a_{nc}/L_{nc} = 4(\rho c\mathcal{D})^{1/2}$] will be dominant at every frequency. The practical values of $\rho, c, \mathcal{D}$ (typically $a_{nc}/L_{nc} \sim 10^{-1}$, which is not very small) may make the observation of these laws uncomfortable. The discussion of the case of the joint effects of diffusion, electrolyte resistivity and Faradaic resistance is done in the Appendix. In this case there are three exponents as the frequency is increased (see Fig. 18). The low-frequency exponent is always $(D-1)/2$ and the high-frequency exponent is 0, but for the intermediate frequencies the exponent may be or not a function of the fractal dimension.

D. Towards a complete description of the Sierpiński electrode

Section IX C has brought together the various elements associated with a Faradaic process. The interface capacitance can be incorporated simply by putting "in parallel" the resulting admittance with the results of Sec. II. Upon increasing frequency, one then generally expects an $\omega^{(D-1)/2}$ regime characteristic of diffusion, then an intermediate regime $\omega^{\eta_{\mathcal{D}S}}$ or ω^{D-2}, depending upon whether series resistance or Faradaic resistance is the first limitation coming in, then an ω^0 regime. The blocking regime $\propto \omega^{\eta}$ is expected to appear at higher frequencies. However, depending upon the system (e.g., concentration of electroactive species), the ω^{η} regime may well wash out

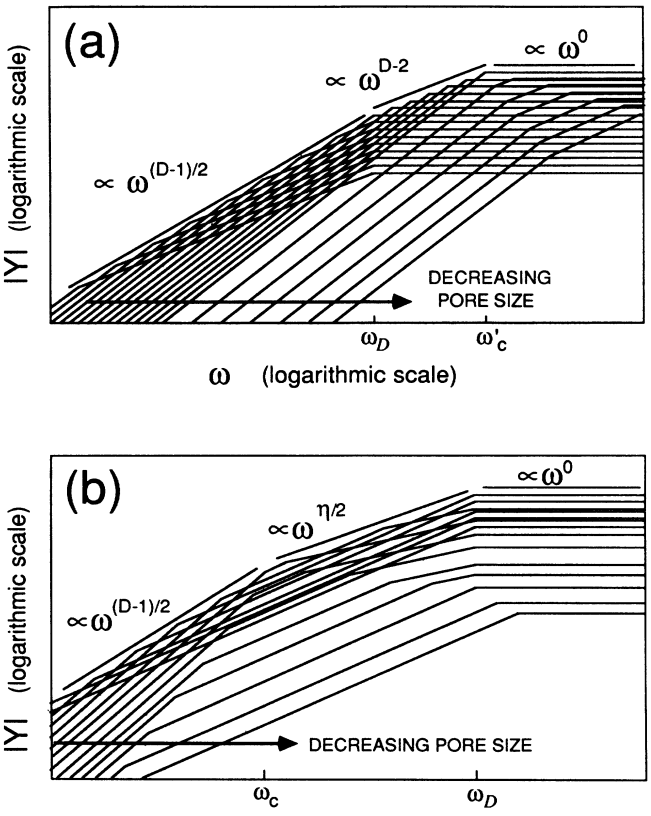

FIG. 18. Bode diagram of the generalized Sierpiński electrode in the diffusive plus Faradaic plus electrolyte resistivity regime. (a) Low-resistivity case $[L^2\rho/r^2c\mathcal{D} \ll (a_0/4rc\mathcal{D})^{2(\ln\alpha_z/\ln\alpha)}]$. Here the two low-frequency exponents both depend directly on the fractal dimension. (b) High-resistivity case $[L^2\rho/r^2c\mathcal{D} \gg (a_0/4rc\mathcal{D})^{2(\ln\alpha_z/\ln\alpha)}]$. Here the low-frequency exponent depends directly on the fractal dimension but at intermediate frequencies a different exponent which is not related to the fractal dimension appears.

one or several of the regimes associated with the Faradaic process. Furthermore, it may occur that η is smaller than $(D-1)/2$. In such a case, the capacitive admittance $\propto \omega^{\eta}$ would reappear at the lowest frequencies. This surprising result may be understood as due to the smallest pores, which give essentially a capacitive contribution.

X. CONCLUSION

Unfortunately, this discussion does not even exhaust the very limited problem of the Sierpiński electrode. All these calculations have been performed assuming that no dc current is flowing in the system, which is far from being the case in most practical situations. The presence of a dc current flowing would make the (potential-dependent) Faradaic admittance vary from one point of the interface to another. This would complicate the problem considerably and most probably the results would be affected. We will not consider this complicated case in this paper. Keeping in mind the linear-response

regime we draw below the principal results of that work.

(1) The frequency response of a porous electrode depends directly on the electrochemical regime.

(2) For parallel structures we have demonstrated that the frequency response of a blocking electrode is of the CPA type but the exponent is not a function of the fractal dimension. The same exponent is, however, conserved in a limited frequency range for a nonblocking electrode. In this situation the value of the exponent depends on the type of hierarchy. This is exemplified by the case of parallel spherical pores (PSP) which possess CPA response when nonfractal and behave like an RC circuit when the surface is fractal.

(3) In the "diffusion" or "diffusion and Faradaic" regimes the response depends directly on the fractal dimension for a fractal surface. This is related to the fact that the physical effects which determine the response are *local* in contradistinction with the high-frequency blocking regime. Two exponents can be found for different frequency ranges.

(4) We recall that diffusion effects can appear only in liquid electrolytes where there exist at least two kinds of mobile ions. They can appear in solid mixed electronic plus ionic conductors. They cannot appear in ordinary solid electrolytes with only one kind of mobile ions.

(5) In general, starting from low frequency a fractal electrode may present a $\eta=(D-1)/2$ regime then followed by a $\eta=D-2$ regime, then followed by a $\eta=0$ regime, itself followed by a regime where the exponent indeed depends on the hierarchy but not through the fractal dimension. At very high frequencies where edge effects are dominant, a last type of exponent may appear which for a generalized Sierpiński electrode is equal to $(\ln N/\ln\alpha)-1$ irrespective of the fractal dimension.

(6) The case of a fractal PSP is a limiting case where the diffusive response would be of the CPA type whereas at higher frequency a simple RC response is obtained.

(7) In all the cases that we have examined the admittance of a fractal electrode is not an extensive quantity: It is not proportional to the macroscopic apparent area of the electrode.

(8) The response is not proportional to the microscopic transport coefficients either. The admittance presents power-law dependences upon electrolyte resistivity, exchange resistance, specific capacitance, diffusion coefficients, and frequency.

(9) A necessary condition to have a CPA response in the parallel scheme is the existence of a "shoulder" in the Bode diagram of one element.

(10) Whatever the electrochemical regime the behavior of a fractal electrode is not related to the smaller details of the geometry in the regime in which it exhibits CPA behavior. In this case the response is governed by pores which have a characteristic size directly related to frequency. Scanning the frequency sweeps various pore sizes of a porous electrode.

(11) We have provided a model for a random porous interface which exhibits CPA behavior. The essential condition is that the hierarchy implies a direct parallel branching of the smallest elements on the largest holes. For this system not all the pores of a given size are equivalent. Only a part of the porous structure intervenes practically in the exchange in the frequency regime where capacitive effects are dominant. In that situation it is not the fractal dimension obtained through a uniform "measure" of the surface which plays a role. The response could perhaps be related to a nonuniform "multifractal" measure or to some definition of the dimension which involves the accessibility. Of course, at very low frequency where diffusion dominates the entire structure participates to the current.

(12) Due to the fact that the response is linear, the admittance of a fractal electrode is an holomorphic function of the frequency. In consequence the small signal dc response is directly related to the small signal ac response, at least in the absence of diffusion effects. All the results that are obtained for the ac response in various geometries in the blocking regime can be connected to the dc response. This permits immediate transposition to the study of constant flux through fractal surfaces, like membranes, lungs alveolas, and plant roots as indicated in Ref. 30.

This is perhaps the most promising aspect of our results that we can condense in the following manner: studying, theoretically or experimentally, the frequency response of an electrode with, rough, porous, or fractal interface is equivalent to the study of the dc flux across the same interface. But as shown in Ref. 30 the problem of the *steady-state* flux of neutral species governed by diffusion in a volume across a membrane of the same geometry is exactly equivalent.

It is then possible that in the future it will be possible to study a number of natural processes occurring in physiology or agriculture by only measuring the frequency dependence of the response of a model electrode of the same geometry.

ACKNOWLEDGMENTS

The authors wish to acknowledge useful discussions with Dr. J. C. Bates, Dr. T. C. Halsey, Dr. M. Keddam, Dr. A. Le Méhauté, Dr. H. Takenouti, Dr. C. Tricot, and Dr. J. C. Wang. Very special thanks are due to J. C. Bates, T. C. Halsey, and J. C. Wang for sending reports of their work prior to publication. Laboratoire de Physique de la Matière Condensée is Unité de Recherche Associée No. 1254 du Centre National de la Recherche Scientifique, France.

APPENDIX

The admittance of a single pore, in the presence of diffusion and Faradaic resistance, has been discussed above. Two cases were considered, depending upon the existence of an $\omega^{1/2}$ region. Now, the inclusion of the series resistance of the electrolyte leads us to considering five cases (1)–(5), shown in Figs. 19(a) and 19(b). Large pores ($a_n \gg 4rc\mathcal{D}$) lead to three regimes in the absence of series resistance, hence cases (1)–(3) depending upon the relative magnitudes of $a_n^2/\rho L_n$ with respect to $4a_nL_n/r$ and $16c\mathcal{D}L_n$. Small pores ($a_n \ll 4rc\mathcal{D}$) do not exhibit the $\omega^{1/2}$ intermediate regime in the absence of series resis-

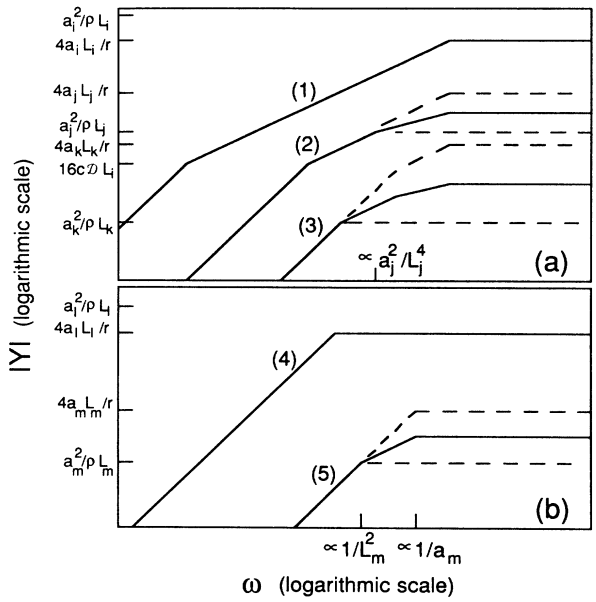

FIG. 19. Bode diagram of single pores in the diffusive plus Faradaic plus electrolyte resistivity regime (low-frequency part). (a) Large pores ($i<j<k$); (b) small pores ($l<m$). These two cases correspond to the two cases of Fig. 15(a), but now with the resistivity of the electrolyte taken into account.

tance, hence only two further cases (4) and (5) depending upon the magnitude of $a_n^2/\rho L_n$ with respect to $4a_n L_n/r$. When the Sierpiński electrode is considered, it appears that, upon decreasing pore size, one will successively meet different cases, from (1) to (5), but two different types of sequences may be encountered.

(i) $(1\rightarrow 4\rightarrow 5)$ if $L_n^2 \ll r^2 c\mathcal{D}/\rho$ when $a_n = 4rc\mathcal{D}$. This will occur if $L^2\rho/r^2 c\mathcal{D} \ll (a_0/4rc\mathcal{D})^{2\ln\alpha_z/\ln\alpha}$. The two regimes of Fig. 15 will then be found. However, a third regime will appear at the higher frequencies, due to the occurrence of case (5) for the smallest pores. The exponent might be determined by the scaling behavior of the $\omega^{1/2}$ to ω^0 crossover point ($\omega \propto 1/a_n, |Y| \propto a_n^{3/2}$), hence an exponent $\ln(N/\alpha^{3/2})/\ln\alpha$. This, however, is negative in the allowed parameter range. One will then simply get a plateau for $\omega > \omega_c' = 4/a_{nc}' cr$ at a value $Y_{\max} \sim N^{n_c'}[4(a_{nc}')^3/\rho r]^{1/2}$, where a_{nc}' is such that $a_{nc}'/(L_{nc}')^2 = 4\rho/r$ [see Fig. 19(a)]. This gives

$$Y_{\max} \sim (4a_0^3/\rho r)^{1/2}(a_0 r/4\rho^2)^{(\ln N - 3\ln\alpha/2)/(\ln\alpha - 2\ln\alpha_z)} .$$

We recover here the value of the pure Faradaic admittance, as found in Sec. VII. It is to be noticed that the pores smaller than a_{nc}' give a negligible contribution to the admittance at all frequencies.

(ii) $(1\rightarrow 2\rightarrow 3\rightarrow 5)$ if $L_n^2 \gg r^2 c\mathcal{D}/\rho$ when $a_n = 4rc\mathcal{D}$, that is if $L^2\rho/r^2 c\mathcal{D} \gg (a_0/4rc\mathcal{D})^{2\ln\alpha_z/\ln\alpha}$. The situation here is more complex, as can be seen in Fig. 19(b). However, only three regimes are found: upon increasing frequency, one successively finds the $(D-1)/2$ regime of diffusion, then a regime determined by the $\omega^{1/2}$ to $\omega^{1/4}$ crossover point of case (2) [the corresponding exponent is $\ln(N\alpha_z/\alpha^2)/2\ln(\alpha_z^2/\alpha) = \eta_{\mathcal{D}S} = \eta/2$], then finally the ω^0 regime. The change from $\omega^{(D-1)/2}$ to $\omega^{\eta_{\mathcal{D}S}}$ occurs for those pores with $a_{nc}/L_{nc} = 4(\rho c\mathcal{D})^{1/2}$ and $\omega_c = 16\mathcal{D}/a_{nc}^2$. The change from $\omega^{\eta_{\mathcal{D}S}}$ to ω^0 occurs for $\omega \sim 1/\mathcal{D}(cr)^2$.

It is to be noticed that the two extreme regimes $\omega^{(D-1)/2}$ and ω^0 are identical in cases (i) and (ii). The distinction occurs because of the intermediate regime, which is governed by the Faradaic resistance in case (i) and by the series resistance in case (ii).

[1]See the review by P. H. Bottelberghs, in *Solid Electrolytes,* edited by P. Hagenmuller and W. Van Gool (Academic, New York, 1978), Chap. 10, and references therein. See also R. de Levie, Electrochim. Acta **10**, 113 (1965).

[2]B. Mandelbrot, *The Fractal Geometry of Nature* (Freeman, San Francisco, 1982).

[3]J. C. Wang and J. B. Bates, Solid State Ionics **18&19**, 224 (1986).

[4]A. Le Méhauté and G. Crépy, Solid State Ionics **9&10**, 17 (1983).

[5]A. Le Méhauté and A. Dugast, J. Power Sources **9**, 359 (1983).

[6]J. B. Bates, J. C. Wang, and Y. T. Chu, Solid State Ionics **18&19**, 1045 (1986).

[7]S. H. Liu, Phys. Rev. Lett. **55**, 529 (1985).

[8]L. Nyikos and T. Pajkossy, Electrochim. Acta **30**, 1533 (1985).

[9]T. C. Halsey, Phys. Rev. A **35**, 3512 (1987).

[10]T. C. Halsey, Phys. Rev. A **36**, 5877 (1987).

[11]T. Kaplan and L. J. Gray, Phys. Rev. B **32**, 7360 (1985).

[12]T. Kaplan, S. H. Liu, and L. J. Gray, Phys. Rev. B **34**, 4870 (1986).

[13]T. Kaplan, L. J. Gray, and S. H. Liu, Phys. Rev. B **35**, 5379 (1987).

[14]M. Keddam and H. Takenouti, C. R. Acad. Sci. Paris **302**, 281 (1986).

[15]B. Sapoval, Solid State Ionics **23**, 253 (1987); R. M. Hill and L. A. Dissado, *ibid.* **26**, 295 (1988); Y. T. Chu, *ibid.* **26**, 299 (1988).

[16]B. Sapoval, J.-N. Chazalviel, and J. Peyrière, in Sixth International Conference on Solid State Ionics, Garmisch-Partenkirschen, 1987 [Solid State Ionics **28-30**, 1491 (1988)].

[17]B. Sapoval, M. Rosso and J.-F. Gouyet, in *Superionic Conductors and Solid Electrolytes: Recent Trends,* edited by A. Laskar and S. Chandra (Academic, New York, in press).

[18]T. Pajkossy and L. Nyikos, J. Electrochem. Soc. **133**, 2061 (1986).

[19]J. B. Bates and Y. T. Chu, in Sixth International Conference on Solid State Ionics, Garmisch-Partenkirschen, 1987 [Solid State Ionics **28-30**, 1388 (1988)]; J. B. Bates, Y. T. Chu, and W. T. Stribling, Phys. Rev. Lett. **60**, 627 (1988). J. B. Bates, Y. T. Chu, and W. T. Stribling, Phys. Rev. Lett. **60**, 627 (1988).

[20]M. Keddam and H. Takenouti, Electrochim. Acta **33**, 445 (1988).

[21]J. C. Wang, in Sixth International Conference on Solid State Ionics, Garmisch-Partenkirschen, 1987 [Solid State Ionics

28-30, 1436 (1988)].
[22]L. Nyikos and T. Pajkossy, Electrochim. Acta **31**, 1347 (1986).
[23]P. G. de Gennes, C. R. Acad. Sci. Paris **295**, 1061 (1982).
[24]R. de Levie, Electrochim. Acta **8**, 751 (1963); **10**, 113 (1965).
[25]C. Grebogi, S. McDonald, E. Ott, and J. A. Yorke, Phys. Lett. **110A**, 1 (1985); **113A**, 495(E) (1986).
[26]C. Tricot, Ann. Sci. Math. Québec **11**, 205 (1987).
[27]C. Tricot, Phys. Lett. **114A**, 430 (1986).
[28]A. Oustaloup, *Systèmes Asservis Linéaires d'Ordre Fractionnaire* (Masson, Paris, 1983).
[29]E. Warburg, Ann. Phys. **67**, 493 (1899); K. J. Vetter, *Electrochemical Kinetics, Theoretical Aspects* (Academic, New York, 1967), Chap. 2; D. C. Grahame, J. Electrochem. Soc. **99**, 370 c (1952).
[30]B. Sapoval, Proceedings of the Seventh International Congress for Stereology, Caen, France, 1987 [Acta Stereologica **6/III**, 785 (1987)].

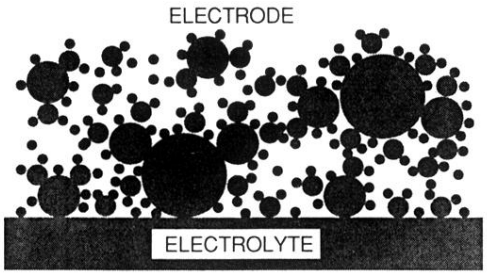

FIG. 11. A quasiporous system build from superposition of hyperbranched spherical pores. All the pores are active in the diffusion regimes described in Sec. IX.

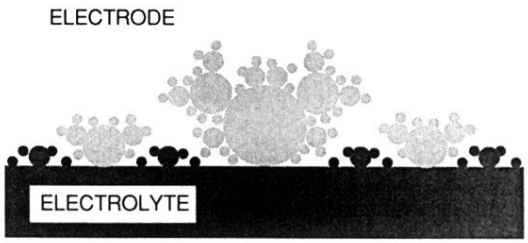

FIG. 12. Possibly active pores of a porous electrode in the blocking or nonblocking regime with no diffusion. This is equivalent to the electrode of Fig. 11 where buried pockets are inactive at all frequencies. Active pores at a given frequency are shown by hatching. Only the regions connected to the external surface through spheroids of size $\leq b_v$ are active at a given frequency. The critical size b_v of the "entry" is proportional to $\omega^{-\ln\alpha/(\ln 2+2\ln N-\ln\alpha)}$.

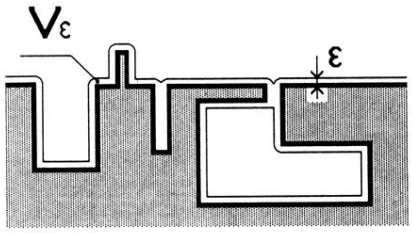

FIG. 5. Definition of the "exterior Minkowsky-Bouligand dimension." The contour of the electrode is the solid line. The electrode is shown in gray. The contour is "fattened" in the electrolyte by taking all the points of distance smaller than ε to the electrode (thin line). The volume $V(\varepsilon)$ is proportional to ε^{3-D} for an ordinary fractal surface.